# Stratigraphy, Depositional Environments, and Reservoir Characteristics of the Tussy (Desmoinesian) Sandstones, Southeast Joiner City Field, Love and Carter Counties, Oklahoma*

Jeffrey M. Cook[1]

Search and Discovery Article #20317 (2015)
Posted July 27, 2015

*Adapted from Oklahoma State University Master of Science Thesis, 2012; manuscript received Jun 25, 2015, accepted July 1, 2015.

[1]Continental Resources, Inc., Oklahoma City, Oklahoma (geojmc@gmail.com)

## Abstract

The Tussy interval of the Desmoinesian Series is defined as the set of strata between the Tussy Limestone at the top and the Upper Dornick Hills Group at the base. Analysis of cross-sections in the study area (in the Marietta Basin) reveals a southerly thickening of the Tussy interval, and rose plots of bedding dips show a dominant north-to-south sediment transport direction. Thus, the basin depocenter was south of the Southeast Joiner City field during Tussy deposition.

The Tussy A and B cored intervals are rocks that were deposited in marine, fluvial, floodplain, and estuarine environments; they show evidence of sea-level cyclicity. Eleven core-derived facies were interpreted, each with distinct sedimentary structures and reservoir quality. Characteristics of the lithotypes from analyses of core, thin-sections, and core-derived porosity and permeability data reveal that grain size, degree of cementation and clay content are the major controls on reservoir quality. The best reservoir facies are of coarser grain size, are poorly cemented, and have small amounts of pore-clogging clays.

The Tussy A and B sandstones were interpreted as meandering stream deposits, composed of amalgamated and laterally connected, side-attached point-bar deposits within a channel (meander) belt. This conclusion is based on sedimentary structures, sand-body geometry and sand-body distribution patterns which resemble modern analogs of meander belts.

## Introduction

### Purpose of the Research

The purpose of this study was to develop a better understanding of reservoir characteristics of the Middle Pennsylvanian Tussy sandstones in Southeast Joiner City field of Love and Carter counties, Oklahoma (Figure 1), and thereby aid in developmental drilling and production-enhancement operations. Interpretation was made of the stratigraphic framework, facies, and depositional environments, as they relate to reservoir quality, along with spatial distribution and connectivity of reservoir rocks. Describing and mapping the stratigraphic variation of these

reservoirs was expected to produce these benefits: enhanced reservoir-management strategies, improved prediction of reservoir properties, increased production, and prolonged life of the field. This study may very well serve as an analog for exploration and development of similar Pennsylvanian sandstone reservoirs.

**General Methods and Data**

To achieve the research objectives, methods employed were:

- Analysis, correlation, and calibration of conventional wireline logs, borehole image logs, and cores--to provide information for interpretation of the stratigraphic framework, facies, and depositional environments, and their relation to reservoir quality. Stratigraphic cross-sections of wireline logs were used to reconstruct the configuration of strata in the study area; they form the basis for determination of reservoir geometry.
- Identification of constituents and porosity types--to determine their controls on reservoir quality.
- Characterization of reservoir geometry, connectivity, and overall reservoir quality through stratigraphic, petrographic, and petrophysical analyses and subsurface mapping.

Subsurface data in the study area consist of two cores (from Hembree 3-17and Gilley 20-2, Figure 2), more than 100 wireline logs, and 11 borehole-image logs. Fifteen thin-sections from one of the cores were analyzed to determine the influence of diagenesis on reservoir quality. Core-derived petrophysical properties were used to relate reservoir quality to lithofacies. Wireline logs were the principal source of information used to depict the stratigraphic and structural frameworks. Available logs rich in information for inferences about lithofacies and reservoir quality are: Extended Range Micro Image (XRMISM) (Halliburton), Electrical Micro Imager (EMITM) (Halliburton), Fullbore Formation MicroImage (FMI) (Schlumberger ®) or Compact™ MicroImage (CMI) (Weatherford).

**Study Area**

The Southeast Joiner City field **(**Figure 2) is a mature oil field in T. 5-6 S., R. 1-2 W, approximately 10 miles southwest of the city of Ardmore and in the central part of the Marietta Basin (Figure 1). The northernmost portion of the study area lies within the North Simon field (Figure 3). Tussy sandstones have produced approximately 5 million stock-tank barrels of oil within the study area. Within the Southeast Joiner City field the Tussy sandstones are unitized and are currently under secondary recovery production enhancement by Mid-Con Energy Operating.

**Previous Work**

Previous works allow for a broad regional overview of the Lower and Middle Pennsylvanian sedimentary rocks of the Marietta Basin, or else they focus on petroleum geology of specific fields. Hoard (1954) detailed the stratigraphy and lithology of the Tussy Sandstone sequence within the “Tussy Sector” of the Tatums field in Carter and Garvin counties. Mullen (1954) provided a stratigraphic, lithological, and structural analysis of the Hewitt field in Carter County, approximately 10 miles north of the Southeast Joiner City study area. Neustadt (1954) analyzed the geologic history and subsurface structure of the West Hewitt field, which is also approximately 4 miles north of the study area. Reeves and

Mount (1960) provided a detailed study of possible oil accumulations along the northern flank of the Marietta Basin and proposed that Pennsylvanian sandstones were/are prime candidates for stratigraphic traps. Westheimer (1965) noted that the Desmoinesian lower Deese sandstones, which include the Tussy, have limited areal extents. Billingsley et al. (1996) interpreted a tidal influence on lower Deese sandstones exposed in the Ardmore Basin, based on bi-directional flow indicators, such as herringbone cross-stratification and flaser to lenticular bedding.

## Geologic Framework

### Regional Structure

The Marietta Basin is a small, northwest-trending structural basin in southern Oklahoma (Figure 1). The study area is in the central portion of the basin, in northern Love and southern Carter counties. The Marietta Basin is bounded by two northwest-trending positive structural features, the Criner Arch and the Muenster Arch. Two major structural features are progressively north of the Criner Arch: the Ardmore Basin and the Arbuckle Mountains, respectively (Figure 1). The Marietta Basin becomes progressively deeper southeast of the study area; this portion of the basin is known as the Gordonville Trough which extends southeastward from Love County into Cooke and Grayson counties, Texas (Bradfield, 1968).

The Ardmore and Marietta basins are within the southeast portion of the southern Oklahoma aulacogen. The southern Oklahoma aulacogen extends from the Ouachita fold belt in southeastern Oklahoma 700 km WNW into southwestern Oklahoma and northern Texas (Feinstein, 1981). He noted similarities in the subsidence curves of the Marietta and Ardmore basins, which support the theory that the basins are two fragments of an original larger basin (Ham et al., 1964). Uplift during Late Mississippian into the Pennsylvanian, during the final deformational stage of the aulacogen, is thought to have been sources of the large volume of sediment in the Ardmore and Marietta basins. Ham et al. (1964) estimated downwarp of the Marietta basin relative to the Muenster Arch was approximately 15,000 ft. The Criner Hills gained approximately 20,000 ft of relief above the surrounding basins during Desmoinesian time (Tomlinson and McBee, 1962).

### Local Structural Geologic Setting and Hydrocarbon Entrapment

Dip within the study area is southwestward, at 600 to 900 ft per mile. Figure 4 shows configuration of the Tussy Limestone (at the top of the Tussy interval) (Figure 5). The Tussy section (175-300 ft thick) unconformably overlies the Desmoinesian Upper Dornick Hills Group. Northward, the Tussy interval pinches out against the Upper Dornick Hills unconformity. Where the sandstones develop good porosity, they form reservoirs that stratigraphically trap hydrocarbons by updip pinchout against the unconformity.

The pre-Pennsylvanian structure within the study area is that of a breached anticline, bounded on the northeast and southwest by normal faults. The structure is essentially an anticlinal horst that trends northwestward. Seismic reflection data would be required to determine accurately the configurations and exact locations of these bounding faults, and currently there is no available evidence that these large-scale faults offset Desmoinesian strata within the study area. The NW-SE anticlinal trend parallels many of the prominent regional structures previously noted. Figure 6 is a Pre-Pennsylvanian subcrop map showing the breached anticlinal structure.

Figure 7 consists of two rose plots of drilling-induced fracture-strike directions from the Hembree 3-17 and PD Sullivan 3-6 borehole image (BHI) logs. The wells are in the southern and northern parts of the study area, respectively. Drilling-induced fractures typically form parallel or subparallel to the maximum horizontal stress direction (Shmax). Analysis of BHI logs reveals a dominant northeastward strike of drilling-induced fractures; the dominant Shmax direction varies between N20E and N60E. Understanding Shmax is important in developmental drilling and enhanced-recovery operations because dominant natural fracture sets typically form parallel to subparallel to Shmax. Analysis of BHI logs has revealed a correlation between Shmax and the orientation of natural fractures. One of the crucial components to well placement within the study area is orienting injector-producer well pairs at least 10 degrees from the Shmax. Doing so decreases the likelihood of early injection water breakthrough from injector to producer wells. Based on analysis of image logs in comparison to other highly fractured reservoirs, these reservoirs are not considered to be intensely fractured, but it is thought that fractures do have an effect on waterflood sweep efficiency and overall reservoir performance.

**Paleogeography**

During Middle Pennsylvanian (Desmoinesian) time, the Marietta Basin was positioned south of the Arbuckle uplift, east of the Wichita uplift, west of the Ouachita uplift and north of the Muenster Arch. Farther north on the Cherokee Platform, in present-day north-central Oklahoma, Desmoinesian deltaic systems (Bartlesville, Red Fork, Skinner, Prue) were dispersing sediment from a northerly source onto the shelf. Figure 8 illustrates a model of early Desmoinesian Midcontinent paleogeography.

**Stratigraphy**

Figure 5 is a typical log for the study area. The Tussy interval is defined as the set of strata between the Tussy Limestone at the top and the Atokan Upper Dornick Hills Group at the base. “This limestone is the key bed used in subsurface work of the Lower Deese Formation in southern Oklahoma” (Hoard, 1954). The Tussy interval is divided informally (in descending order) into: Tussy A, B, and C (Figures 5 and 9), representing three cycles of shale-sandstone-shale. The top of the Tussy interval, marked by the Tussy Limestone, is easily identifiable in the subsurface on wireline logs by its distinct gamma-ray and bulk density signature. The Tussy A Sandstone is fine-grained, and its gamma-ray signature is bell-shaped (Figure 5). Tussy B consists of two sandstones; the lower typically is very fine-grained commonly with a funnel-shaped gamma-ray signature, whereas the upper Tussy B Sandstone has a bell-shaped gamma-ray character (Figure 5). Tussy C consists of a sandy limestone conglomerate that is almost certainly ubiquitous within the study area (Figure 5). Mudstones are developed between the Tussy A, B and C sandstones. The base of the Tussy interval unconformably overlies the Desmoinesian Upper Dornick Hills. The interval shows a southerly (basinward) thickening. Rose plots of cross-bedding from two borehole image (BHI) logs (Figure 10) infer a dominant southerly sediment transport direction, also inferred from southerly planar lamination dips for the Tussy A and B sandstones in Hembree 3-17 (Figure 11).

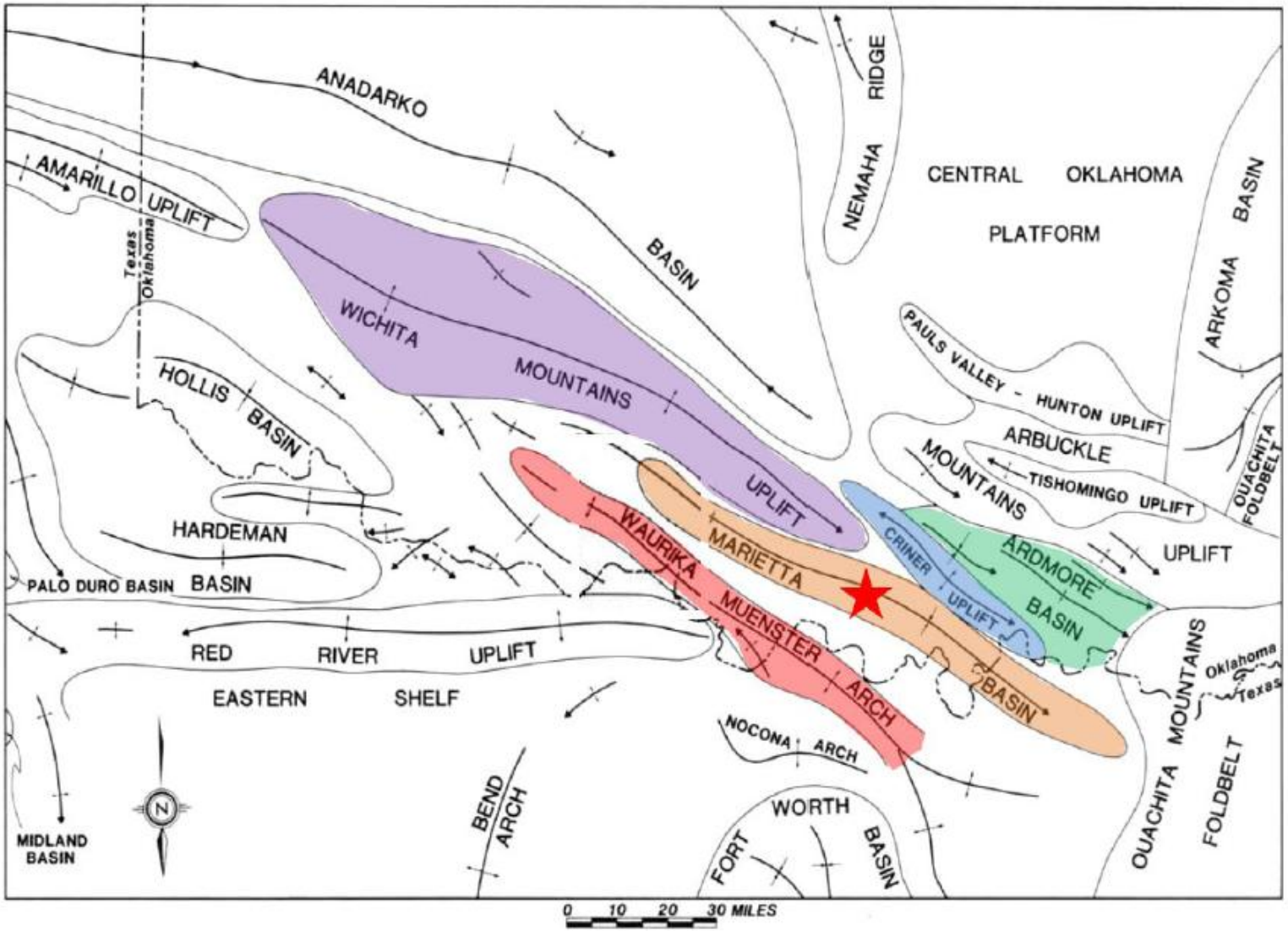


Figure 1. Map of southern Oklahoma and north Texas showing the location of the study area (red star) relative to prominent tectonic features. Marietta Basin – orange, Criner Uplift – blue, Ardmore Basin – green, Wichita Uplift – Purple, Waurika-Muenster Arch – red. (Modified after Al-Shaieb et al., 1980.)

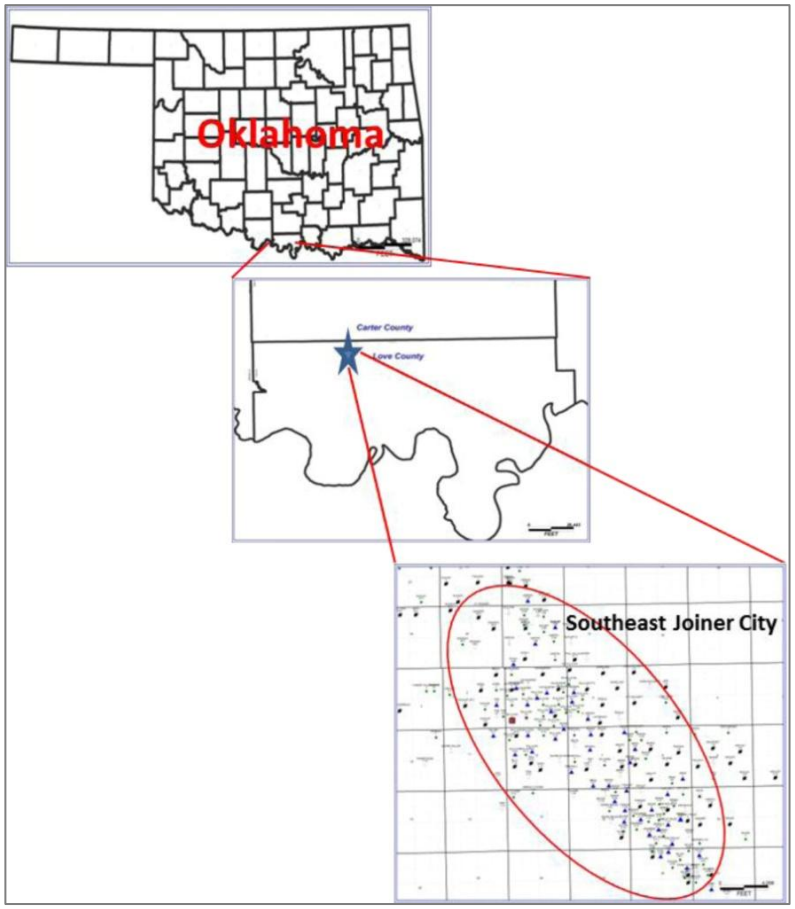


Figure 2. Location map of study area, Southeast Joiner City field in Love and Carter counties, Oklahoma, with location of key wells Mid-Con Energy Operating Inc., Hembree 3-17 (Sec. 17, T. 6 S., R.1 W.) and Santa Fe Minerals Inc., Gilley 20-2 (Sec. 20, T. 6 S., R.1 W.).

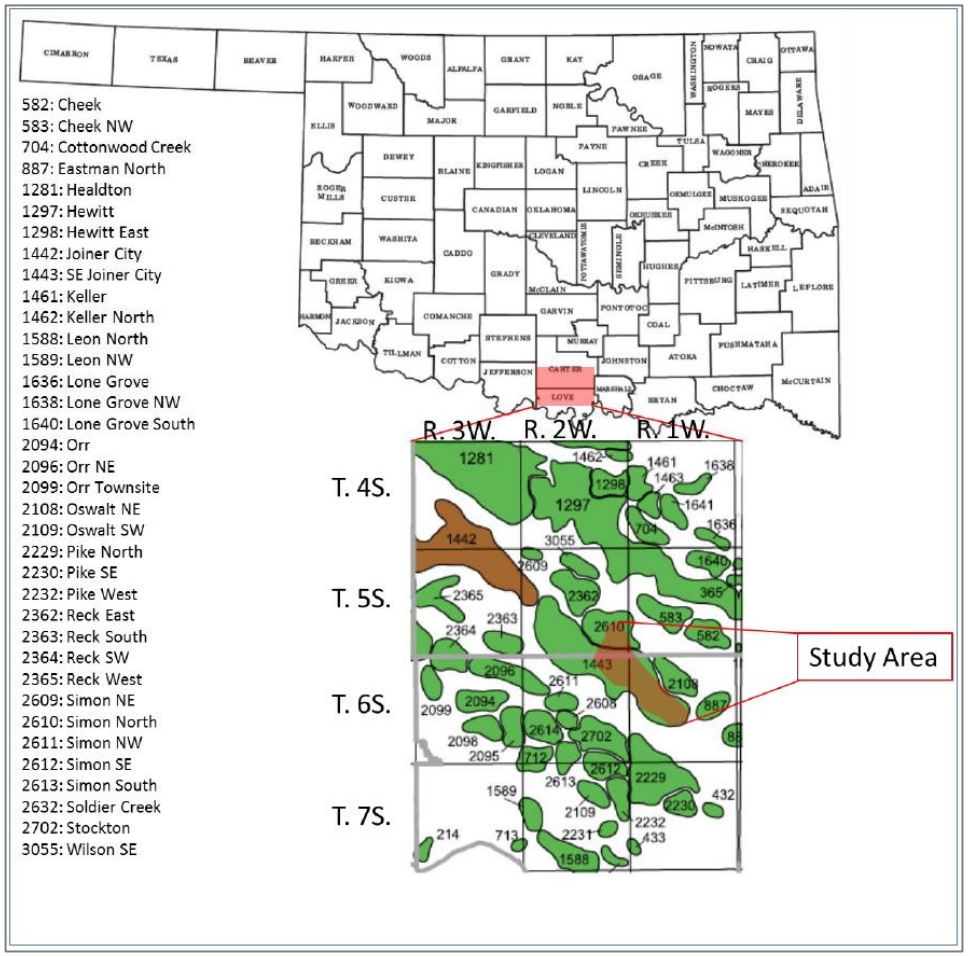


Figure 3. Map of Oklahoma showing the location of the Southeast Joiner City field and study area relative to surrounding oil fields (with list of field names) in northern Love and southern Carter counties (modified from Boyd, 2002).

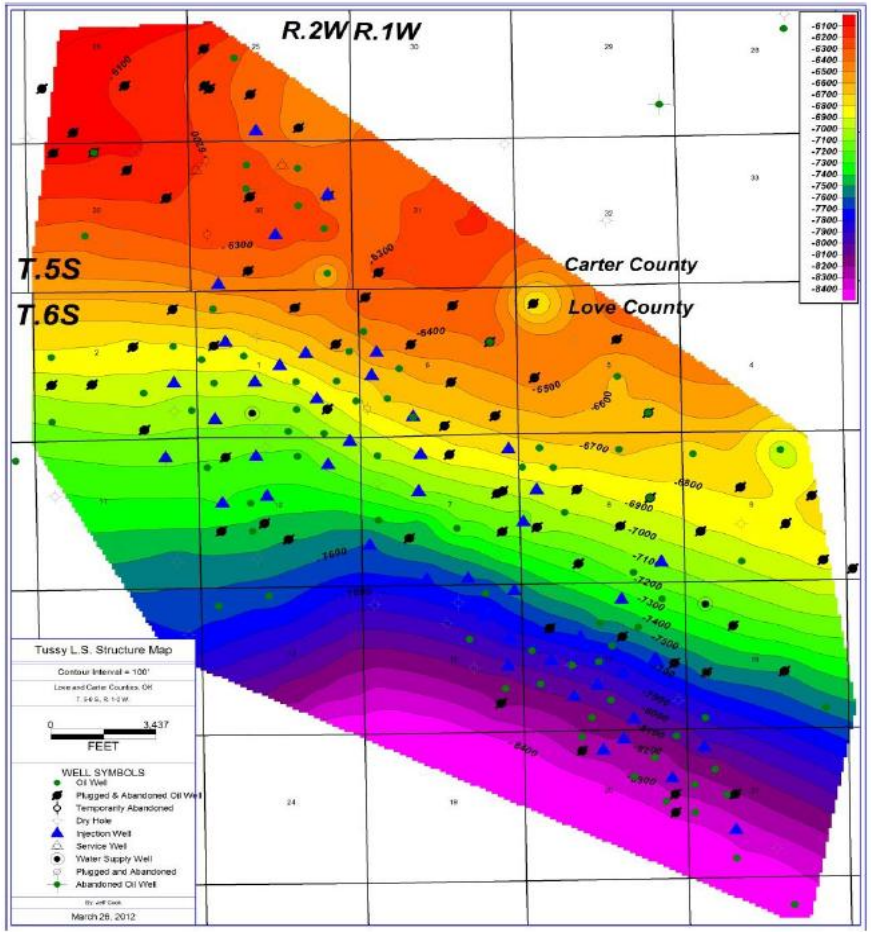


Figure 4. Structural contour map, Southeast Joiner City Field, on the top of the Tussy interval within the study area, showing southerly dip associated with the S.E. Joiner City anticline. Depths relative to sea level are shown in color scale bar; depths range from -6400 ft (red) to -8100 ft (purple).

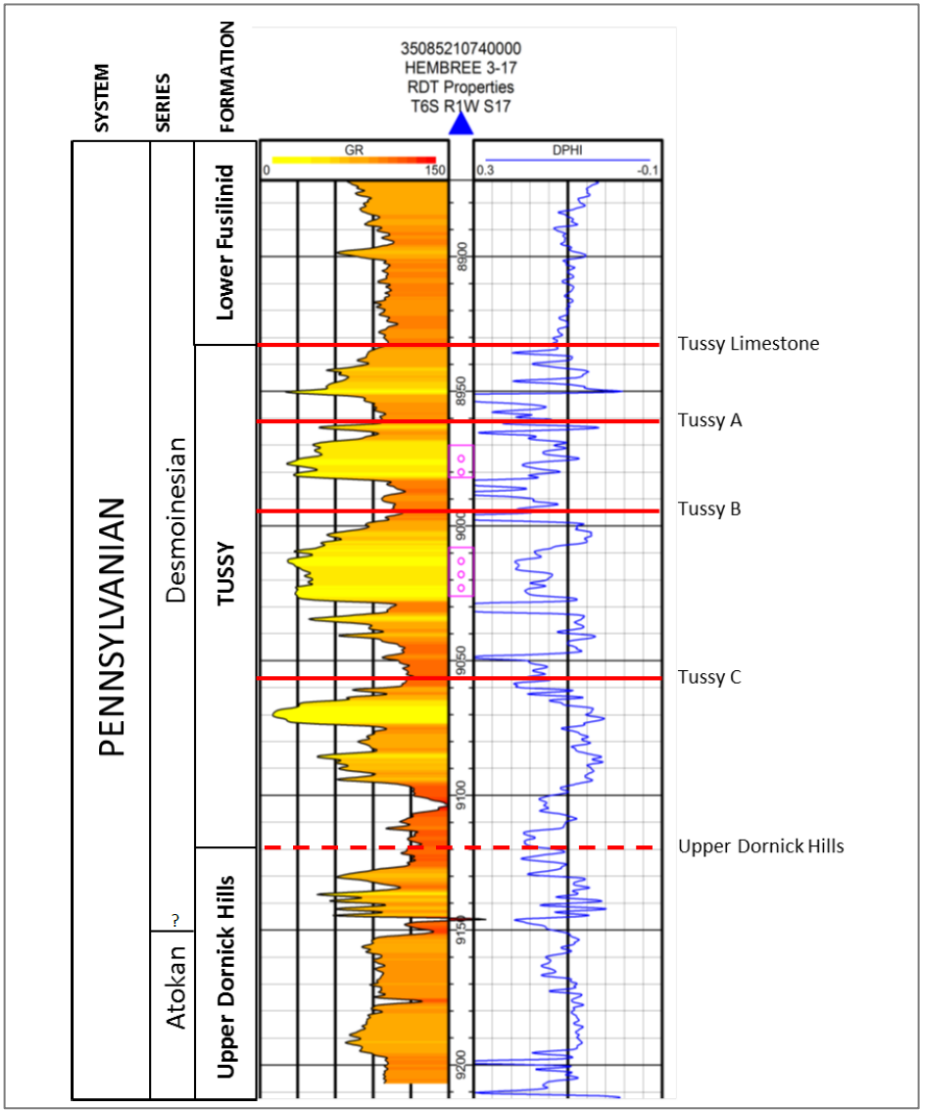


Figure 5. Type log including the Tussy interval, NE. Oswalt Field, Marietta Basin (RDT Properties, Hembree 3-17. Gamma-ray (GR) values increase from yellow to orange and density porosity (DPHI) is shown in blue on the right track.

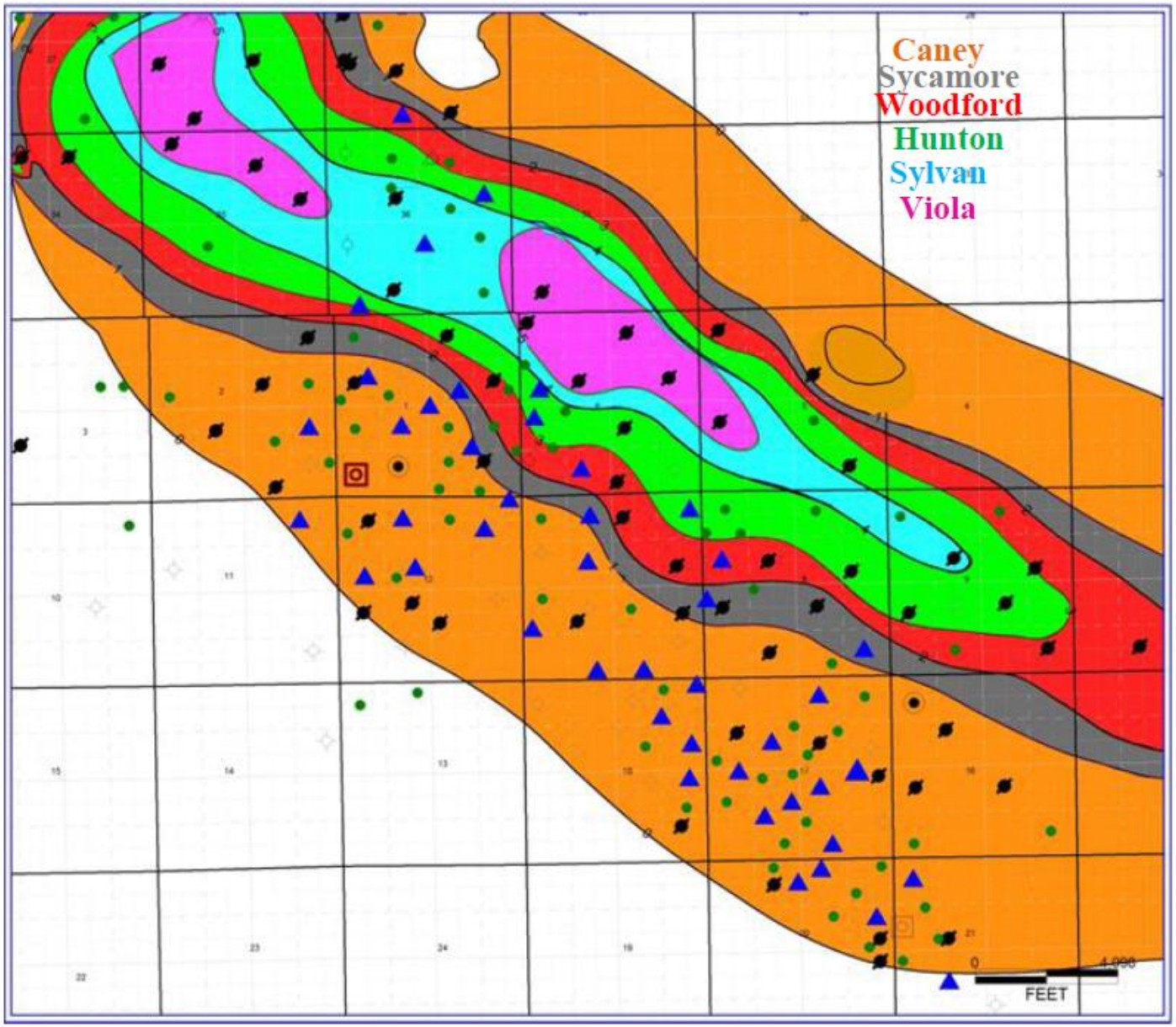


Figure 6. Paleogeologic map of pre-Pennsylvanian strata, showing evidence of a breached anticline within the study area (Abbott, 2006).

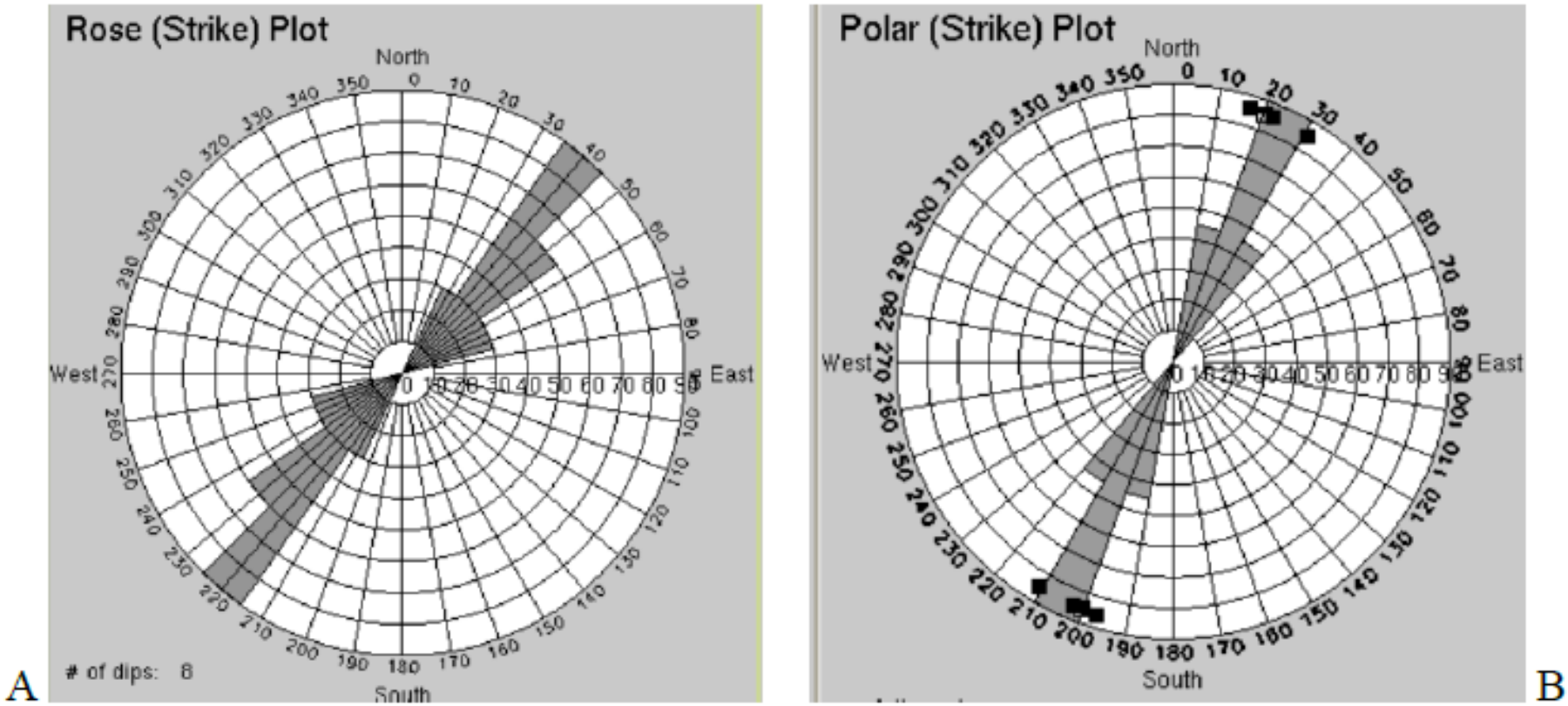


Figure 7. Rose plots of drilling-induced fracture and maximum horizontal stress directions from the Hembree 3-17 (A) and P.D. Sullivan 3-6 (Sec. 6, T. 6 S., R.1 W.) (B) XRMI borehole image logs. Both sets of data were acquired by Halliburton and interpreted by R. Montalvo (Hembree 3-17) and J. Mitchell (P.D. Sullivan 3-6) (Halliburton borehole-image interpreters).

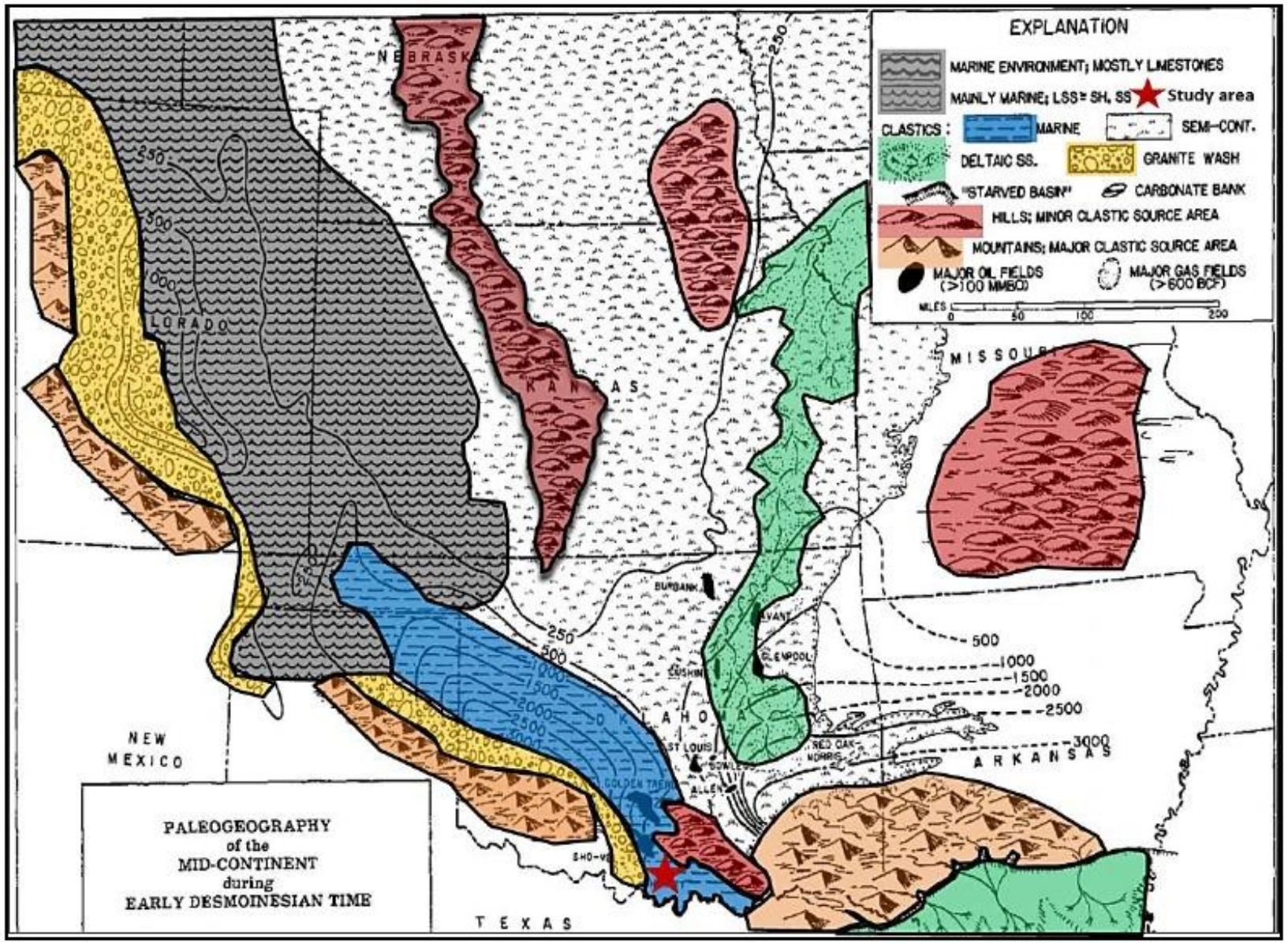


Figure 8. Paleogeography of the Mid-Continent during early Desmoinesian time, showing thickness of early Desmoinesian rocks (modified after Rascoe and Adler, 1983).

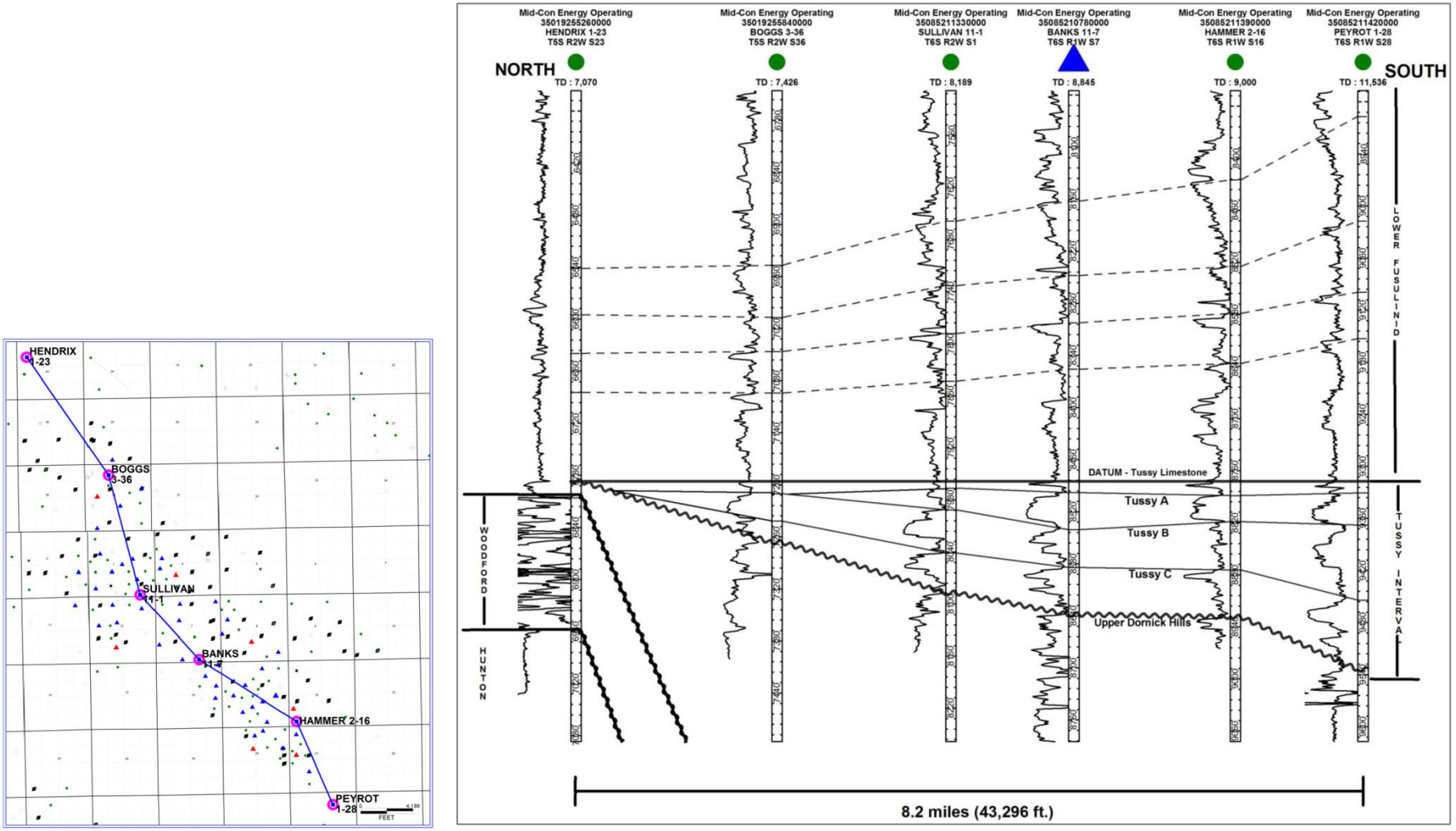


Figure 9. North-to-south gamma-ray log cross-section, with location map, through the study area. The Tussy interval is bounded above by the Tussy Limestone and below by the Upper Dornick Hills Limestone. Datum is the top of the Tussy interval, marked by the Tussy Limestone. Northward from the Mid-Con Sullivan 11-1, exact stratigraphic relationships within the Tussy interval are not known, due to unavailability of critical data.

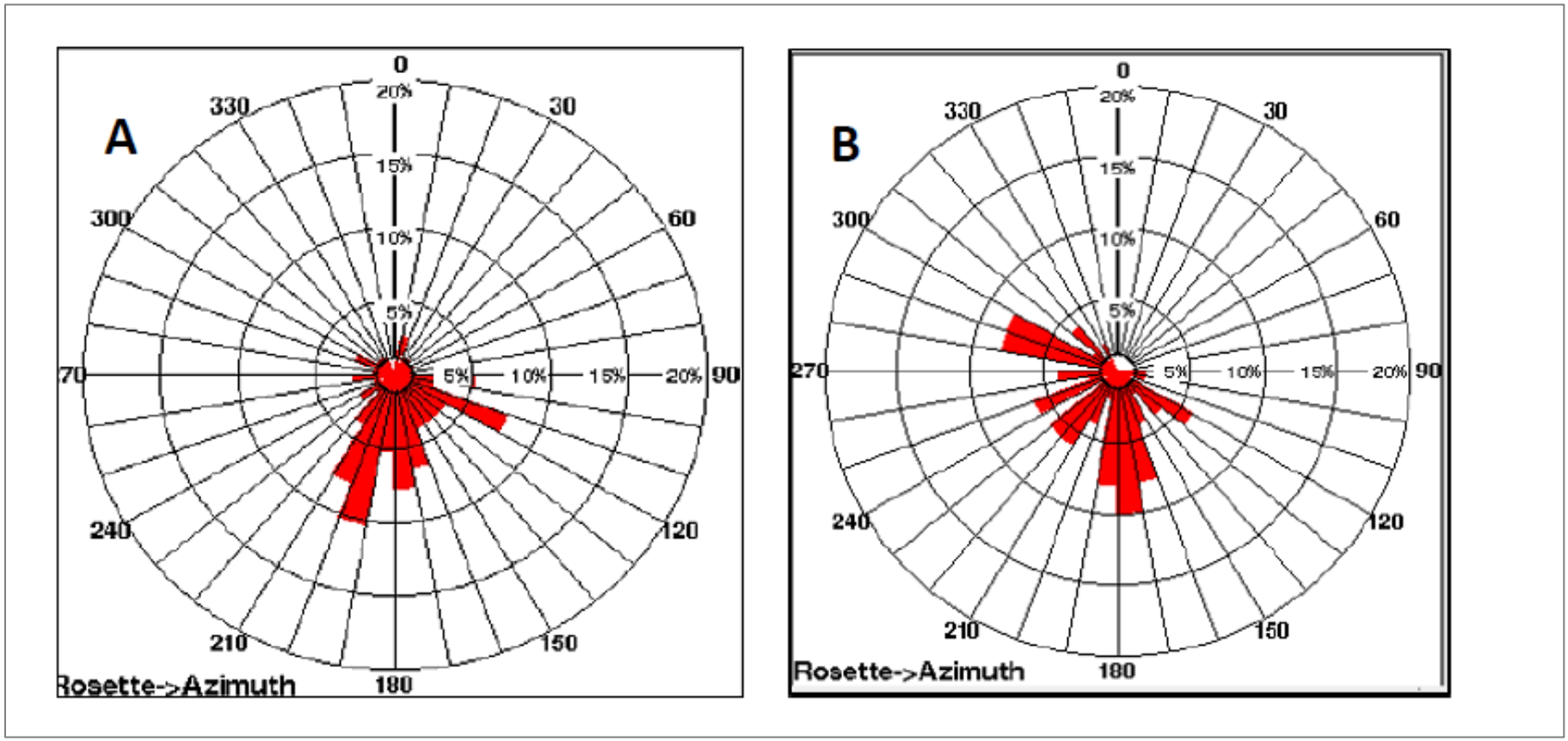


Figure 10. Rose plots of cross-bedding dips within the Tussy interval from (A) Elaine 3-18 (Sec. 18, T. 6 S., R.1 W.) FMI and (B) Banks 11-18 (Sec. 18, T. 6 S., R.1 W.) FMI. These plots show predominant north-to-south orientation of cross-beds. Both sets of data were acquired by Schlumberger and interpreted by Y. Chen (Schlumberger Borehole Geologist).

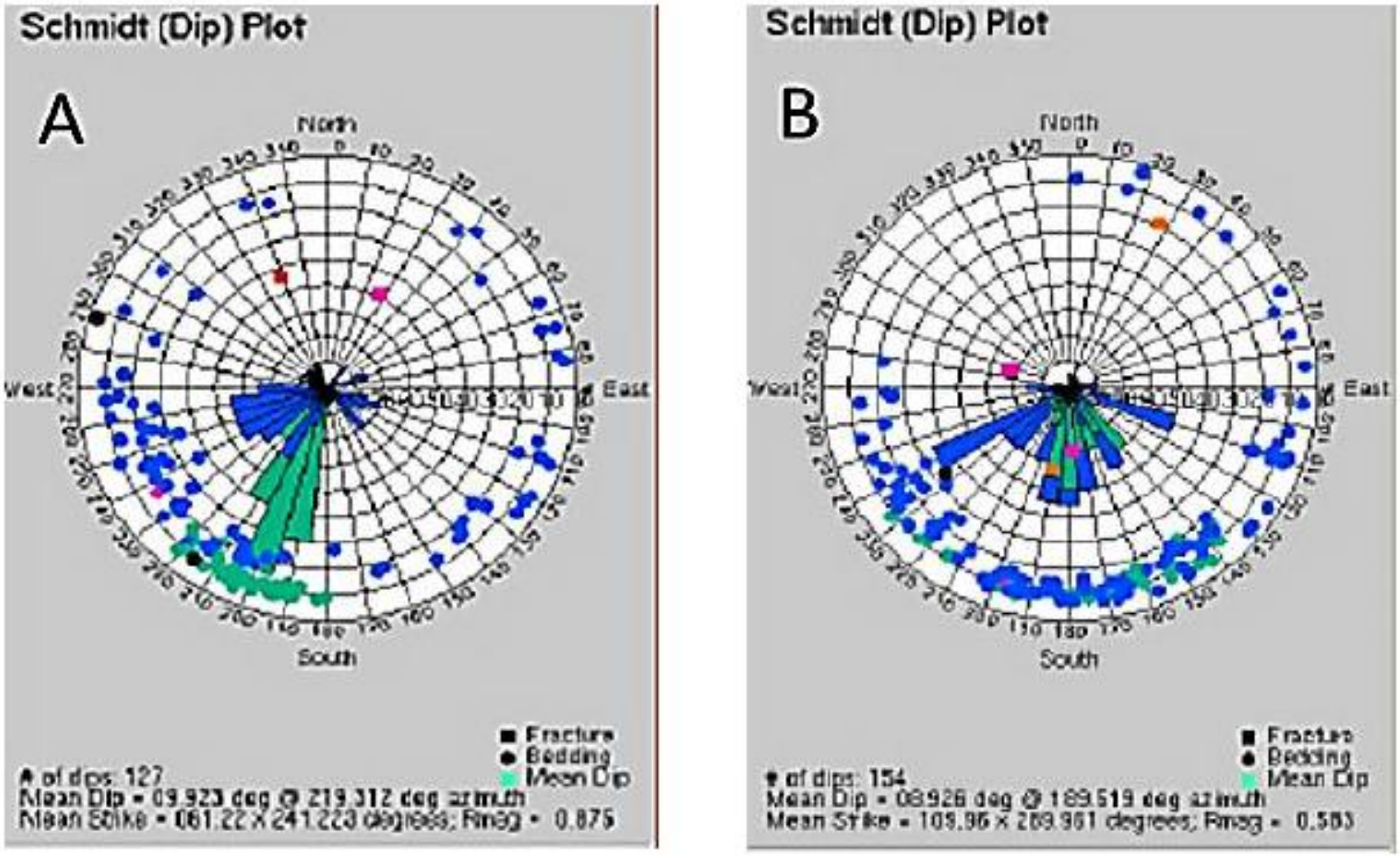


Figure 11. Rose plots from the Hembree 3-17 XRMI, showing orientations of sedimentary dips (primarily cross-bedding) (blue) and planar lamination dips (primarily in mudstones) (green) of (A) Tussy A and (B) Tussy B intervals. Both sets of data were acquired by Halliburton and interpreted by R. Montalvo (Halliburton borehole-image interpreter).

## Petrography, Facies Analysis, and Reservoir Quality

### General Core Description

The Hembree 3-17 core is from the Tussy A and B intervals, whereas the Gilley 20-2 core is of the Tussy A and the uppermost part of the Tussy B interval. In detailed core examination, eleven depositional facies were recognized in the Tussy A and B intervals; they indicate primarily deposition in a fluvial environment.

The Tussy A and B intervals (Figures 12, 13, 14, and 15) are composed of amalgamated fining-upward sets of beds; the sets are capped by current-rippled laminae. The Tussy B Sandstone overlies grey silty mudstone; it consists of fine- to medium-grained, horizontal planar-laminated, cross-laminated, and current-rippled sandstones. The uppermost part of the Tussy B interval contains calcium carbonate and an oxidized zone, indicative of exposure. The Tussy A overlies variegated mudstones with an erosional contact. It consists of fine- to medium-grained, horizontal planar-laminated, cross-laminated, and current-rippled sandstones. The interval above the Tussy A Sandstone was not cored.

### Facies Analysis

Detailed facies recognized in core examination, stratigraphically from older-to-younger strata, are:

**(F1) Clay-clast Conglomeratic Sandstone**
Grey to brown, fine-to-medium-grained conglomeratic sandstone contains abundant subangular to subrounded clay and dolomitized clay rip-up clasts (2-35 mm). F1 is well cemented by calcium carbonate. Bedding is hardly distinguishable. F1 is the lowermost channel-fill. The dominant framework grains are quartz and dolomite, whereas metamorphic-rock fragments, chert, and feldspars are minor constituents. Primary porosity was occluded by calcium carbonate cement and pseudomatrix, with few secondary pores. Reservoir quality is inferred to be poor.

**(F2) Horizontal Planar-laminated Sandstone**
Brown. fine- to medium-grained sandstone is characterized by distinct planar laminae (Figure 16A) . Dark brown laminae are the coarser, being composed of medium-sized grains; whereas the light brown laminae are fine-grained. It is interpreted as the product sheet-like flow within a fluvial channel. Average core-derived porosity and permeability are 15.5% and 96 md, respectively. It is not present in the Hembree 3-17 cored interval

**(F3) Cross-laminated Sandstone**
Brown, fine- to medium-grained sandstone is dominated by dark, inclined laminae (Figure 16B). Coarser grained laminae are dark brown, whereas finer laminae are light brown. It probably formed as dunes. It typically overlies F2 and underlies F4 at some localities and F5 at others. Where F2 is not present, F3 directly overlies F1. Quartz is the dominant framework grain; metamorphic rock fragments, chert, and feldspars compose the minor fraction. Where present, grain-coating illite prohibits quartz overgrowths. In core plug at depth of 8984.7 ft., porosity is 15.8% and air permeability is 131 md. Primary porosity is common, as is secondary porosity, with moldic and oversized pores.

**(F4) Trough Cross-laminated Sandstone**

Brown, very fine- to fine-grained sandstone with foreset laminae. The laminae are curved to planar, consistent with trough cross-bedding in migratory dunes, possibly on point bars of fluvial channels. At depth of 9027.35 ft in the Hembree 3-17, the net confining stress (NCS) is 6500 psi), porosity is 13.2%, and air permeability is 0.783 md. Fine to very fine grain size is consistent with the low permeability (<1 md) measurements.

**(F5) Deformed Sandstone**

Brown, fine-grained sandstone with deformed to convolute bedding and abundant carbonaceous debris. The deformed bedding is irregular to convolute, with sparse fluid-escape structures, due to slumping of unstable channel walls, as well as liquefaction. These features with persistent layers of organic debris are common near the bases of infilled channels (Coleman and Prior, 1981). It typically is underlain by well organized cross-bedded F3 and overlain by very fine-grained, current-rippled F6 facies. Porosity is a combination of primary intergranular porosity and secondary porosity developed by dissolution of feldspar, rock fragments, detrital clay matrix, and diagenetic clays. Pseudomatrix formed by clay is common. Secondary pores are intragranular, moldic, and oversized. At depth of 8980.65 ft in the Hembree 3-17 is a measured NCS of 6500 psi, porosity of 14.2% and air permeability of 2.28 md.

**(F6) Current-rippled Sandstone**

Very fine-grained, silty, brown-to-light-brown, ripple-laminated sandstone is characteristic of F6. Ripples are asymmetrical (unidirectional), penetrated by rare vertical burrows, with few mud drapes. Rippled foresets are commonly 0.5 – 1cm in scale. It is interpreted as unidirectional current deposit in a fluvial channel as the current waned. Unidirectional flow and uniform lithology suggest fluvial channel, not directly affected by tidal processes. Dominant framework constituent is quartz; the minor fraction consists of feldspar, chert, metamorphic rock fragments, and sedimentary rock fragments. Diagenetic constituents include quartz overgrowths and grain-coating illite. Pore space was reduced by abundant pore-clogging pseudomatrix and clays. Both primary and secondary porosity is present.

**(E) Current-rippled siltstone**

Grey to light gray, wavy-laminated to current-rippled siltstone contain abundant “vertical” burrows and carbonaceous clay debris. E is thought to have been deposited during periods of channel flooding, during abandonment, initiated by rise in sea level. It may represent estuarine conditions; it typically is near the top of the sandstone “package” and overlies F6 and underlies paleosol facies P. Framework grains are dominantly quartz, with smaller quantities of feldspar, chert, sedimentary rock fragments, and metamorphic rock fragments. Detrital clay matrix occludes porosity. Reservoir quality is poor.

**(P) Paleosol**

Grey-to-dark-grey siltstone to very fine-grained sandstone has a red-to-orange, crumbly oxidized character in localized nodules and vertically aligned irregular fractures – a pedogenic aspect. P is interpreted to have formed during a lowered sea level, with subaerial exposure of an underlying estuarine facies. Thus P is likely the subaerially exposed upper portion of E. It is a non-reservoir, due to its clay- and silt-rich composition.

**(FP) Variegated Mudstone**

Variegated mudstone is crumbly, grey-green-red mudstone. This facies contains sparse thin, dark grey layers of shale. It is interpreted as the product of deposition on a floodplain that was exposed by lowered sea level, associated with activation of the Tussy A fluvial system, in which floodplain muds were later incised by the Tussy A fluvial channels. This sharp and erosional contact is evident in the Hembree 3-17 and Gilley 20-2 cored intervals. Borehole-image (BHI) logs throughout the study area also portray this contact to be abrupt.

**(M1) Silty Mudstone**
Grey silty mudstone with siderite concretions is the main feature. The concretions are interbedded with thin, wispy to inclined, lenticular-bedded to rippled, very fine-grained sandstone. It is interpreted as having been deposited as delta-front; its gamma-ray values diminish upward, implying an upward increase in grain-size. The interbedded sandstones are interpreted as the record of pulses of sediment discharge from the delta mouth. The Tussy B interval in the Hembree 3-17 BHI contains M1 that is overlain sharply by F1.

**(M2) Mudstone**
Dark grey, poorly indurated crumbly mudstone with few siderite concretions (3.5-5cm in thickness) with abundant carbonaceous plant debris characterize M2. The siderite is sub-parallel to bedding. M2 was observed only in the Tussy B cored interval in the Hembree 3-17. It probably was deposited in the distal subaqueous delta plain, representing the most seaward extent of the delta system, as suggested by Boggs (2006).

**Summary of Facies Analysis**

The eleven depositional facies within the Tussy A and B stratigraphic intervals described from the Hembree 3-17 and Gilley 20-2 cores are summarized in Table 1 and illustrated in Figures 12, 13, 14, and 15. The Hembree 3-17 core (Figures 12 and 13) is composed of fluvial facies (F1, F3, F4, F5 and F6), paleosol facies (P) and marine facies (M1 and M2). The Gilley 20-2 core (Figures 14 and 15) is composed of fluvial facies (F2, F3, F4, F5 and F6) and floodplain facies (FP).

**Facies Associations**

**Floodplain**
The floodplain association consists of variegated grey-green-red mudstone. Floodplain facies was observed in the Hembree 3-17 and Gilley 20-2 cored intervals above the Tussy B Sandstone (Figure 15). This facies is thought to be the result of a lowered sea level, which rejuvenated the Tussy fluvial system. It overlies estuarine facies and is overlain, with an erosional contact, by Tussy A fluvial sandstones.

**Estuarine**
The estuarine facies association consists of a heavily burrowed, current-to-wavy-rippled dark grey, very fine-grained sandstone and siltstone that overlies fluvial facies F6 (Figure 12). The main evidence for interpretation is burrows. The uppermost part of the estuarine facies is an oxidized sediment, associated with pedogenic processes after lowered sea level and consequent exposure of the estuarine facies.

**Fluvial Channel**
The fluvial channel facies association represents the reservoir units in the Tussy interval. It is an overall fining-upward succession of facies. Strata of channel-fill origin are multistoried (each increment 5-30 ft thick) successions of amalgamated fining-upward sequences. Fining-upward sequences have basal erosional surfaces. The internal amalgamated cross-laminated sandstones and scour surfaces are regarded as the record of stacked, lateral-accretionary point-bar deposits. Bases of fluvial channels show abrupt, erosional contacts with underlying mudstone; they are characterized in the lower part by carbonaceous clay-clast conglomeratic sandstone. The sandstones represent channel-fill deposits. The main reservoirs facies are in the lower to middle portions of fluvial channels. Fluvial channel-fill deposits capped by wavy-laminated to unidirectional-rippled siltstone with vertical burrows represent the onset of sea-level rise and the beginning of estuarine depositional processes.

**Marine**

The marine facies association is dark grey mudstone with siderite concretions and carbonaceous plant debris, overlain by grey to dark grey, silty mudstone. The mudstone grades upward into thin, interbedded, wispy parallel-to-inclined siltstone and rippled, very fine-grained sandstone with few vertical burrows and siderite concretions. Data compiled from cores seem to indicate a subaqueous delta-front or prodelta as the depositional setting.

**Controls on Reservoir Quality**

As discussed above, rocks of relatively high porosity and permeability are in the channel facies. Characteristics of these lithotypes from analyses of core, thin-sections, and core-derived porosity and permeability data reveal that grain size, degree of cementation, and clay content are the major controls on reservoir quality. The best reservoir facies are coarser and are poorly cemented, with small amounts of pore-clogging clays. Cross-plots of permeability and porosity show that depositional facies is another control on reservoir quality. The highest permeability is in the laminated and cross-laminated sandstone facies F2 and F3. The highest recorded permeability and porosity, 148 md permeability and 17.7 % porosity, respectively, are in the cross-laminated facies F3 in the Gilley 20-2.

**Summary**

The Tussy A and B cored intervals were deposited in marine, fluvial, estuarine, and floodplain environments; they show evidence of sea-level cyclicity. Tussy A and B sandstones are interpreted to have been deposited in fluvial channels; these fluvial channels consist of successions of amalgamated fining-upward sequences.

Tussy B fluvial processes seem to have thrived during a relative sea-level lowstand. This lowstand is evidenced by the sharp contact between the Tussy B channel base and underlying marine sediments. As sea-level rose, channel abandonment occurred due to decreased fluvial energy. As sea-level continued to rise, the fluvial system diminished to form an estuary with increased biotic activity, evidenced by heavily burrowed siltstone facies. When sea level began to fall, previously deposited estuarine facies were subaerially exposed, as evidenced by paleosol above Tussy B Sandstone. With continued lowering of sea level, Tussy A fluvial system was activated; channel sands were deposited over and incised into floodplain facies. Another rise in sea-level probably shut down the Tussy A fluvial system.

High-quality reservoir rocks are restricted to channel facies. F2, F3, and F5 have the best reservoir quality, whereas F4 and F6 have fair reservoir quality. Primary porosity is common; secondary porosity is primarily from dissolution of feldspars and rock fragments. Pores are intergranular, intragranular, moldic and oversized. Reservoir quality is controlled by grain size, depositional facies, and degree of cementation. The best quality reservoir facies are fine- to medium- grained sandstones with minimal cementation.

## Wireline-Log Signatures

Figure 17 illustrates the interpreted facies from gamma-ray signatures in the Hembree 3-17, after calibration of log to core. The channel facies is displayed as sharp-based, fining upward, bell-shaped gamma-ray curves. Stacked internal fining-upward gamma-ray sequences are shown by successions of fining-upward gamma-ray signatures. The uppermost part of the sandstone body, reflecting channel abandonment/estuarine environment, typically has relatively high GR values. Marine facies lie below the Tussy B channel facies coarsen upward and are funnel-shaped on the gamma-ray log (Figure 17). Floodplain facies between the Tussy B and Tussy A channel-fill facies also has relatively high gamma-ray values.

## Borehole-Image Analysis

High-quality BHI data permits accurate interpretation: orientations of strata, facies (Table 2), composition, texture, degrees of cementation, reservoir quality, faults, fractures, and borehole breakouts. Correlation of a core-calibrated micro-image log to other wells with BHI logs but with no cores allows identification of reservoir facies. Analysis of dipmeter data further helps in defining components of the channel deposits and their geometry (Figure 18).

### Borehole-image Facies Associations

Four borehole-image facies can be correlated on a field-wide scale: (1) fluvial facies, (2) channel abandonment-estuarine facies, (3) floodplain facies and (4) marine facies. The sandstone (reservoir) is underlain by marine mudstones and overlain by abandoned-channel facies and estuarine facies.

### Reservoir Quality

Reservoir quality can be inferred in borehole image logs by analysis of chromatic variation (Devries, 2005). Yellow-to-light-orange hue on the static image indicates good reservoir quality and porous-sandstone facies (more than 10% porosity). Light-orange-to-orange hue typically is associated with very-fine-grained silty to shaly sandstone, of fair to poor reservoir quality (less than 8% porosity). Dark-orange-to-brown hue is associated with silt to mudstone (non-reservoir quality).

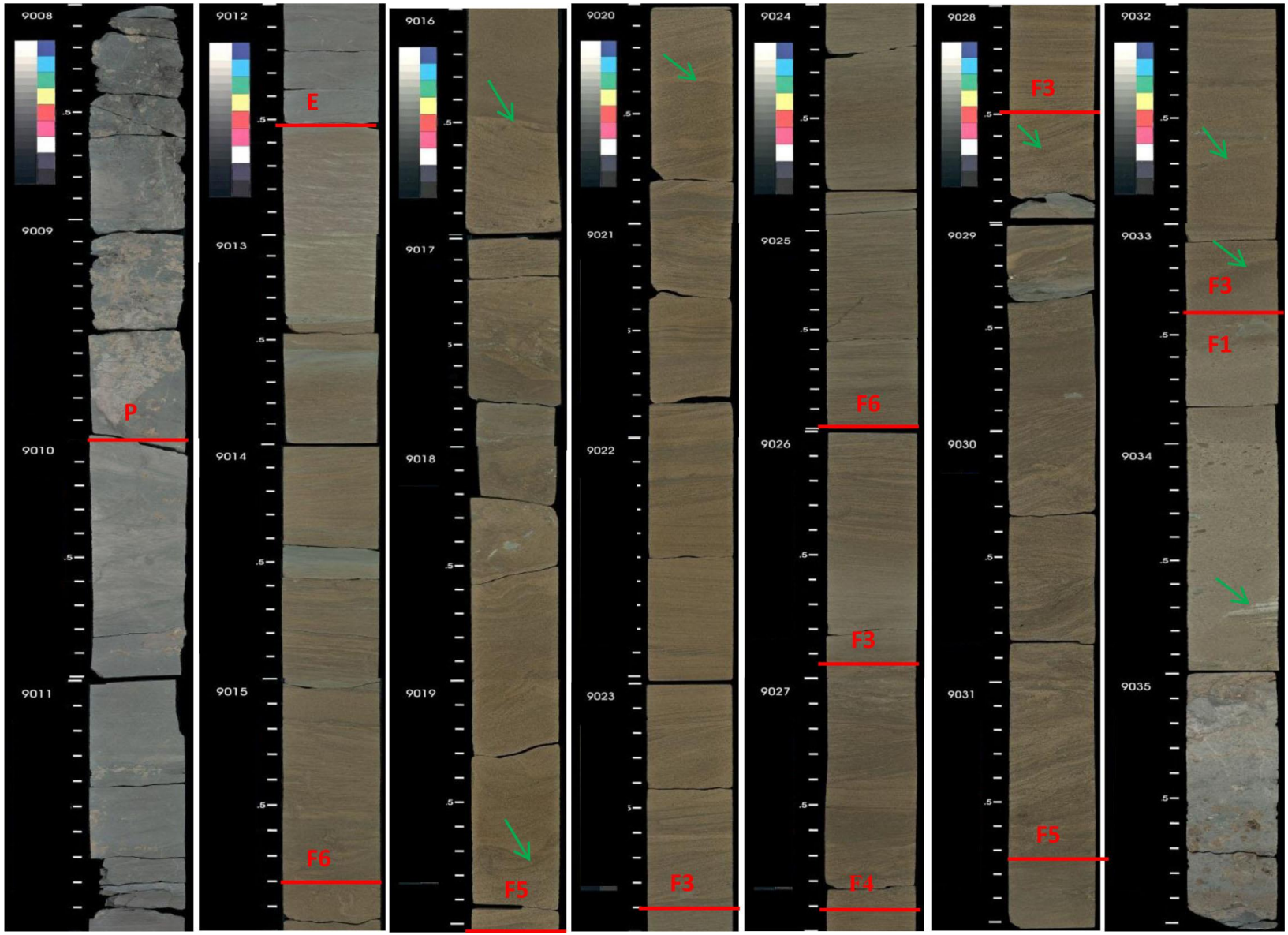


Figure 12. Tussy B Sandstone, Hembree 3-17, showing lithofacies, indicated in red (see Table 1 for codes of facies). Green arrows point to prominent channel reactivation surfaces.

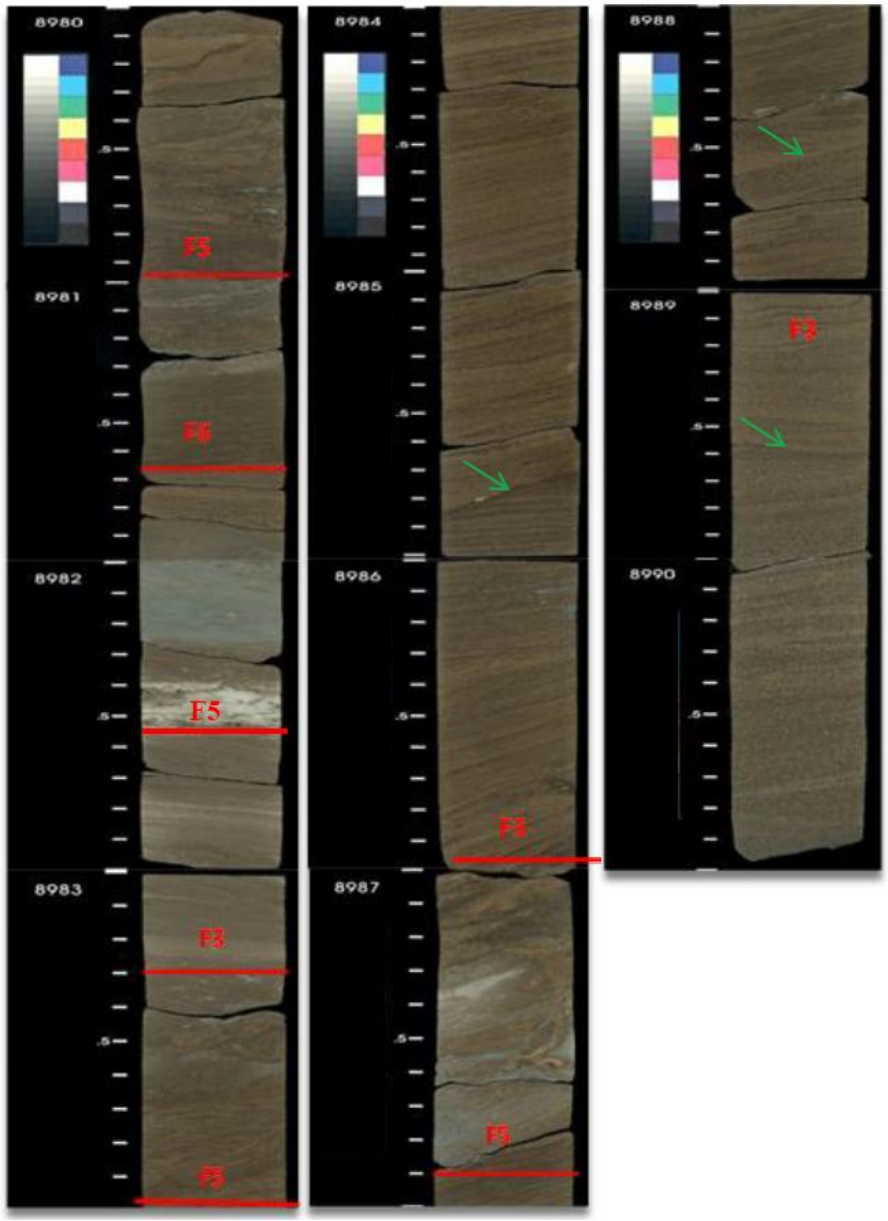


Figure 13. Tussy A Sandstone, Hembree 3-17, showing lithofacies, indicated in red. Green arrows point to prominent channel reactivation surfaces. See Table 1 for codes of facies.


Figure 14. Tussy A Sandstone, Gilley 20-2, showing lithofacies, coded in red. See Table 1 for codes of facies

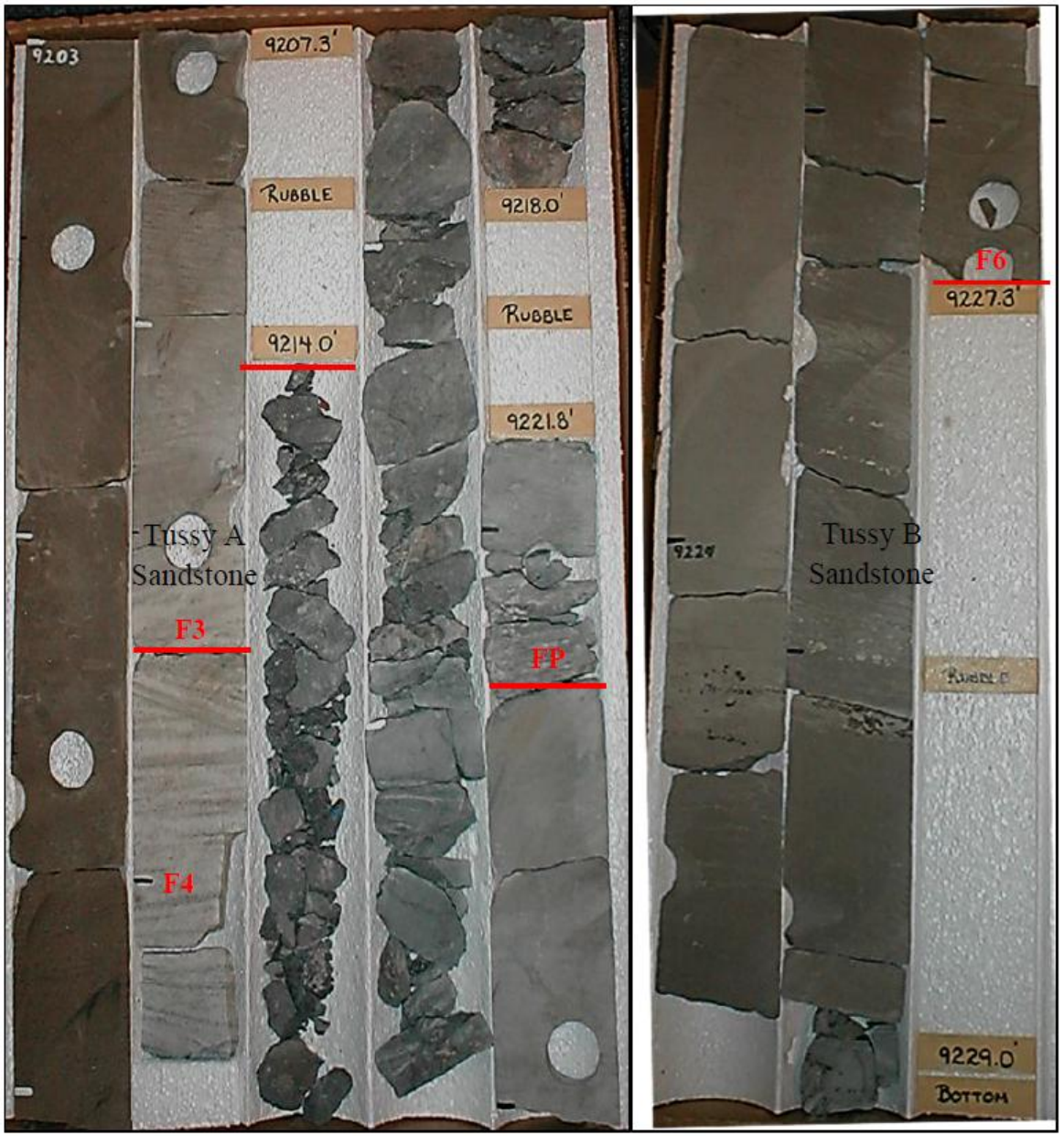


Figure 15. Basal part of Tussy A Sandstone, mudstone below Tussy A Sandstone and uppermost part of Tussy B Sandstone from the Gilley 20-2. Lithofacies indicated in red. See Table 1 for codes of facies.

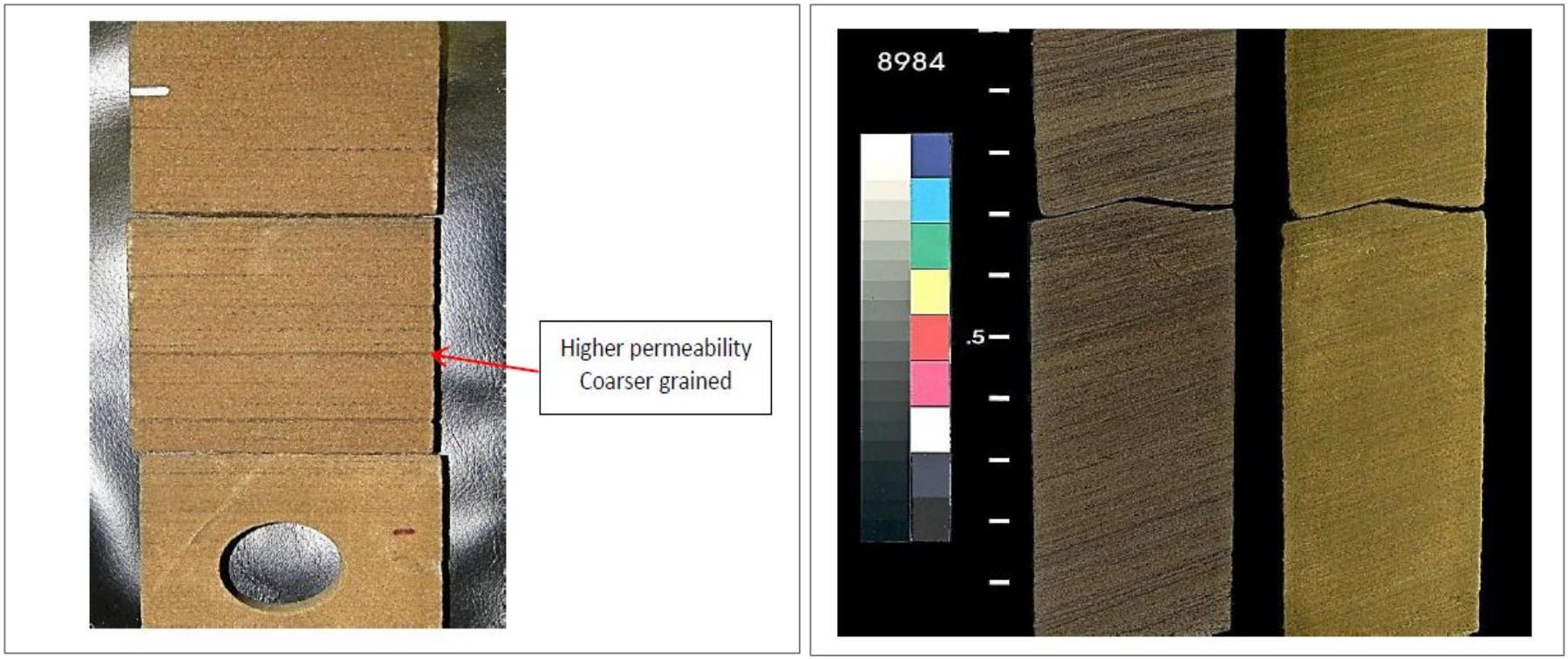


Figure 16. (A) F2 facies from Gilley 20-2. Planar laminations in the sandstone are conspicuous. Depth 9047 feet. (B) Facies F3 from Hembree 3-17. Cross-laminations in the sandstone are conspicuous. Depth 8984 feet.

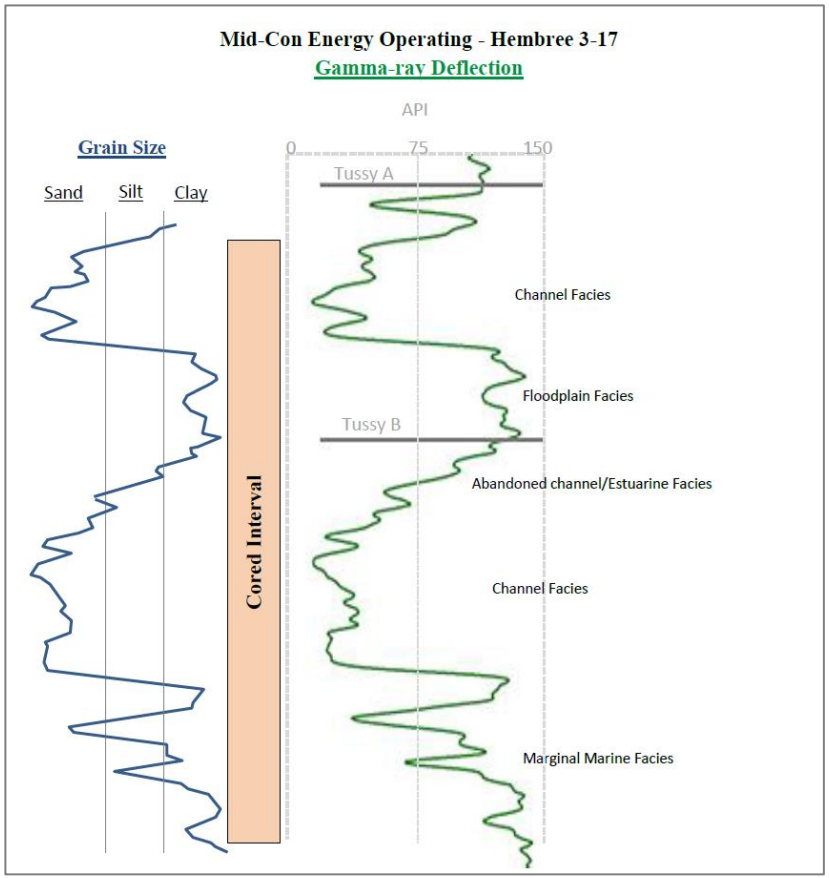


Figure 17. Gamma-ray (green) signatures and generalized grain size of the Tussy A and B cored intervals: Marine, channel, estuarine and floodplain-paleosol facies, Hembree 3-17.

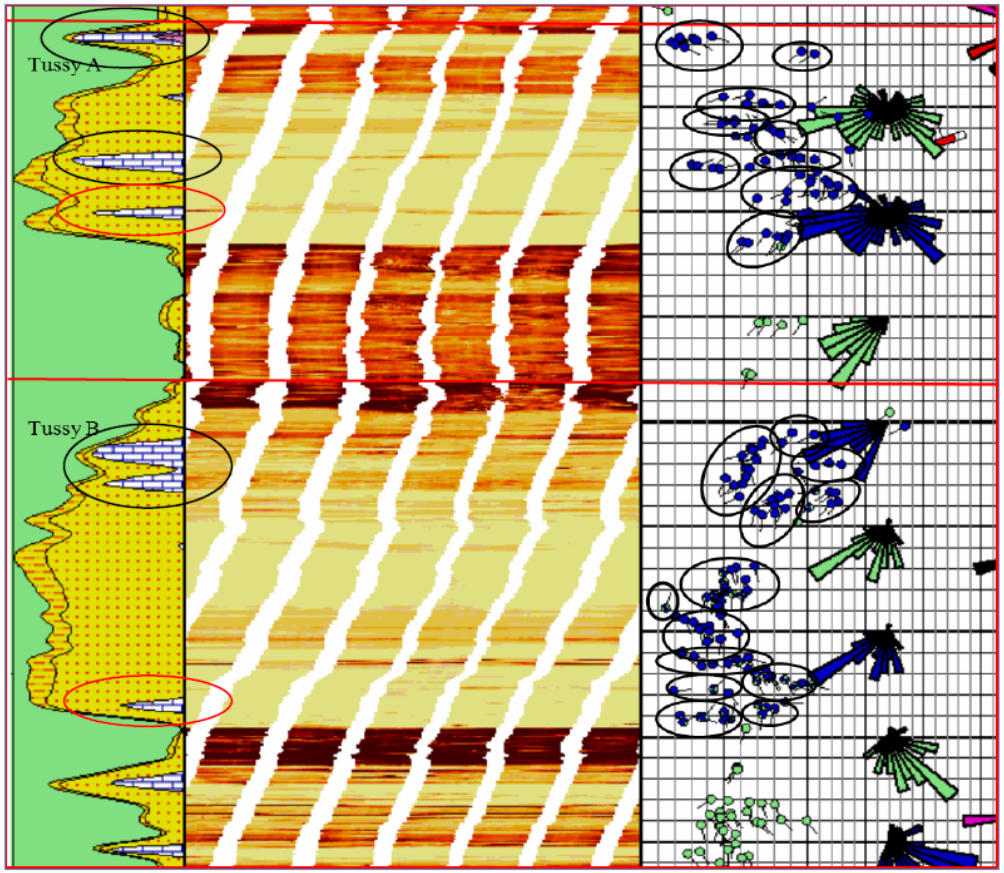


Figure 18. Gamma-ray (left), static image (middle), and sedimentary dipmeter plots (right) from Hembree 3-17 XRMI. Dipmeter tadpoles are grouped into packages of common “unidirectional” dip orientations, interpreted as lateral accretion of stacked fluvial point bars, within a meandering fluvial system. The carbonate present in the middle-to-upper portions of the channel facies (black ovals) are probably a result of groundwater circulation and/or subaerial exposure, whereas the carbonate near the base (red ovals) are probably the result of erosion into underlying carbonate-rich mudstone.

| Facies Code | Facies Name | Grain Size | Dominant Features | Depositional Processes |
|---|---|---|---|---|
| **Fluvial (F)** | | | | |
| **F1** | Carbonaceous clay-clast conglomeratic sandstone | Matrix-supported paraconglomeratic | 1 – 5 cm diameter mud clasts, poorly sorted | Scour and fill |
| **F2** | Horizontal planar laminated sandstone | Fine to upper fine | Horizontal laminations | Unidirectional traction flow |
| **F3** | Cross-laminated sandstone | Fine to upper fine | Low-angle laminations | Alternating between bedload and suspension |
| **F4** | Trough-cross stratified sandstone | Very fine to fine | Trough-cross-laminae | "Unidirectional" to traction flow |
| **F5** | Deformed sandstone | Very fine to upper fine | Deformed/convoluted beds, flow structures | Channel fill slumping |
| **F6** | Current-rippled sandstone | Very fine | Asymmetrical climbing-ripple laminations, few burrows | Current-dominated, traction flow |
| **Estuarine (E)** | | | | |
| **E** | Current-rippled to wavy laminated siltstone | Fine | Current-rippled to wavy laminae, heavily burrowed | Mixed fluvial-marine Estuarine processes |
| **Paleosol (P)** | | | | |
| **P** | Paleosol | Very fine | Crumbly, oxidized material | Subaerially exposed estuarine facies |
| **Floodplain (FP)** | | | | |
| **FP** | Variegated Mudstone | Mudstone | Variegated material (red-green-grey) | Exposed floodplain |
| **Marine (M)** | | | | |
| **M1** | Interbedded silty mudstone and sandstone | Silty mudstone | Silty mudstone interbedded with wavy to discontinuous thin beds (1-3 cm) of siltstone to very-fine sandstone | Marginal-marine, delta-front |
| **M2** | Mudstone | Mudstone | Dark grey mudstone with carbonaceous plant debris | Marine, Pro-delta |

Table 1. Designation of the eleven depositional facies, their characteristic features, and interpreted depositional environments described from cores from Mid-Con Energy Operating Inc., Hembree 3-17 (Sec. 17, T. 6 S., R.1 W.) and the Santa Fe Minerals Inc., Gilley 20-2 (Sec. 20, T. 6 S., R.1 W.) wells.

| FACIES<br><br>Terminology | Borehole Image Characteristics<br><br>Descriptions |
|---|---|
| **F1** | Highly resistive (yellow to orange) interbedded, with resistive (dark orange to brown) clay rip-up clasts. Recognizable on the dynamic or Horiz7 images. Dip meter typically shows "random" tadpoles. |
| **F3** | Highly resistive (white to orange) with sinusoidal pattern from low-angle planar laminae. Recognizable on the dynamic or Horiz7 image. Dip-meter tadpoles show a unidirectional pattern. |
| **F4** | Highly resistive (white to orange to dark orange). Difficult to identify on static and dynamic images due to inconsistency of patterns. (Dipmeter did not record orientations over this interval in the Hembree 3-17.) |
| **F5** | Highly resistive (yellow to orange) with slightly less resistive drapes (orange dark orange). Recognizable on dynamic or Horiz7 images; poorly visible on static image. Dip-meter typically shows unidirectional dip pattern. |
| **F6** | Highly resistive (yellow to orange) with well-defined stacked, rippled laminae sets. Recognizable on dynamic or Horiz7 images; poorly visible on static image. Dip meter typically shows unidirectional dip pattern. |
| **P-E** | Moderately to highly conductive (orange to dark orange). Typically forms the uppermost parts of fining-upward sequences. |
| **M-FP** | Highly conductive (dark orange to dark brown). |

Table 2. Characteristics of facies in Hembree 3-17, as displayed on the borehole-image log.

## Spatial Characteristics of the Reservoirs

### Net-Porous-Sandstone Maps

Net-porous-sandstone isopach maps of the Tussy A (Figure 19) and Tussy B (Figure 20) reservoirs were hand contoured and then digitized into Petra Geological software. The maps illustrate distribution of the reservoirs. The net-porous-sandstone cutoffs used to define the Tussy A and B reservoirs are:

1. (volume of shale less than 40
2. density-porosity more than 12% (with assumed matrix density = 2.71 grams/cm$^3$).

Widths of the Tussy A and Tussy B channels range from approximately 2000 ft. to 4500 ft. (Figures 19, 20, 21, and 22). As interpreted from currently available well logs and derived data, the Tussy A and B reservoirs are about 4 to 6 miles long. The sandstones almost certainly are of significantly greater length. Analysis of Tussy Sandstone production history for the majority of wells in the Southeast Joiner City field shows that reservoirs in the more prolific wells (more than 50,000 barrels of oil) are greater than 8 ft. in thickness. Channel thickness ranges from 1 ft. at the edges to 30 ft. near the center.

### Storage Capacity (phi x h) Maps

Storage capacity of the Tussy A and B sandstones, shown in Figures 21 and 22, respectively, is the product of average porosity and net pay thickness, as calculated for the majority of wells in the study area. These maps were constructed using Petra Geological Software. As expected, the geographic trends are similar to those of the isopach maps, and the locations of greater capacity correspond to thicker reservoir.

### Depositional Model and Meander-belt Analogs

Sedimentary structures, their sequence, gamma-ray log signatures, and geometries of reservoir sandstone, along with borehole imagery and dipmeter data, support a fluvial origin of the Tussy A and B sandstones. Distribution and geometry of the Tussy sandstones (Figures 19, 20, 21, and 22) resemble analogs of meander-channel belts.

Figure 23 is a computer simulation of the distributions and geometries of salient features within a meander belt. It was of value in visualizing prominent depositional features and their relationships. The sandstone bodies form elongated shoestring-like bodies that are oriented generally perpendicular to the depositional strike; this is consistent with meandering fluvial channel geometries described by Cant (1982). In the meander belt computer simulation in Figure 23, numerous abandoned point bars are at the edges of the main meander belt; this pattern resembles “pods” of sandstone shown in the Tussy A and Tussy B isopach maps (Figures 19, 20, 21, and 22).

### Channel Connectivity

Figure 24 illustrates two isopach-map scenarios of meandering-point-bar deposits, from the Miocene Huesca Fan at Ebro, Spain (Donselaar and Overeem, 2008); they show how point bars can be connected by channel-floor sandstone bodies. This research is important for oil-and-gas operators who develop fields composed of (meandering) point bars because these types of deposits are commonly considered to be discontinuous – an attribute that is especially problematic in waterflooding and other enhanced recovery procedures. Point-bar connectivity of similar kind is suspected to be operative in Tussy reservoirs. During enhanced-recovery operations, injection of water has stimulated producing wells that are more than 1 mile from the injection-well. Injector –producer communication is more apparent where both wells are near to the center of the channel belt. However, in a few areas, injector and

producer wells within the same stratigraphic interval are not connected, a fact that is apparent from analysis of detailed injection and production data. For example, Figure 25 is a well-log cross-section that shows evidence of flow barriers between two wells completed in the Tussy A Sandstone. The large volume of water injected (more than 550,000 bbl) into Tussy Sandstone in the Sabre Operating Tom 1-2 has caused no apparent increase in oil or water production in the RDT Tom 3-2, located only 900 feet to the southeast. The unavoidable conclusion is that in this case, sandstones of the point-bar system are isolated.

## Conclusions

This study of Lower Desmoinesian Tussy Sandstone reservoirs in the Southeast Joiner City field in Love and Carter counties, Oklahoma, has the following conclusions:

- Rose diagrams of sedimentary bedding-plane dips indicate a dominant southerly transport toward the depocenter south of the Southeast Joiner City oil field..
- Lithofacies of the Tussy interval are of marine, estuarine, fluvial and floodplain environments. Vertical stacking patterns reveal cyclic deposition that is suggestive of deposition controlled by changes in sea level.
- The Tussy A and B sandstones are interpreted as laterally amalgamated and connected, side-attached point-bar deposits within a channel belt, based on sequence of sedimentary structures and sand-body geometry.
- In context of sequence stratigraphy, lowstand is represented by erosive channel base, followed by fluvial sand deposition and a later slow rise in sea level, represented best by estuarine deposition, culminating in marine deposition. The subsequent lowstand is represented by paleosols and renewed incision by fluvial channels.
- Tussy point-bar fluvial facies (horizontal planar-laminated and cross-laminated sandstone) are the best reservoirs; they show the highest porosity (12% - 18%) and permeability (1md - 148 md).
- Primary porosity and secondary porosity are both common, with the latter having developed from dissolution of feldspar, rock fragments, and detrital clay matrix.
- Core-calibrated conventional wireline logs and borehole-image logs, in more detail, accurately display signatures that correspond to channel-belt, estuarine, and marine facies. The latter are particularly helpful in estimating depositional facies, grain size, and reservoir quality in wells unaccompanied by cores.
- Dipmeter data from borehole-image logs provide evidence about paleocurrents and sand trends.
- Fluid transmitted from one point bar to another is thought to be associated with channel-floor sandstones that connect adjacent point bars during their migration.

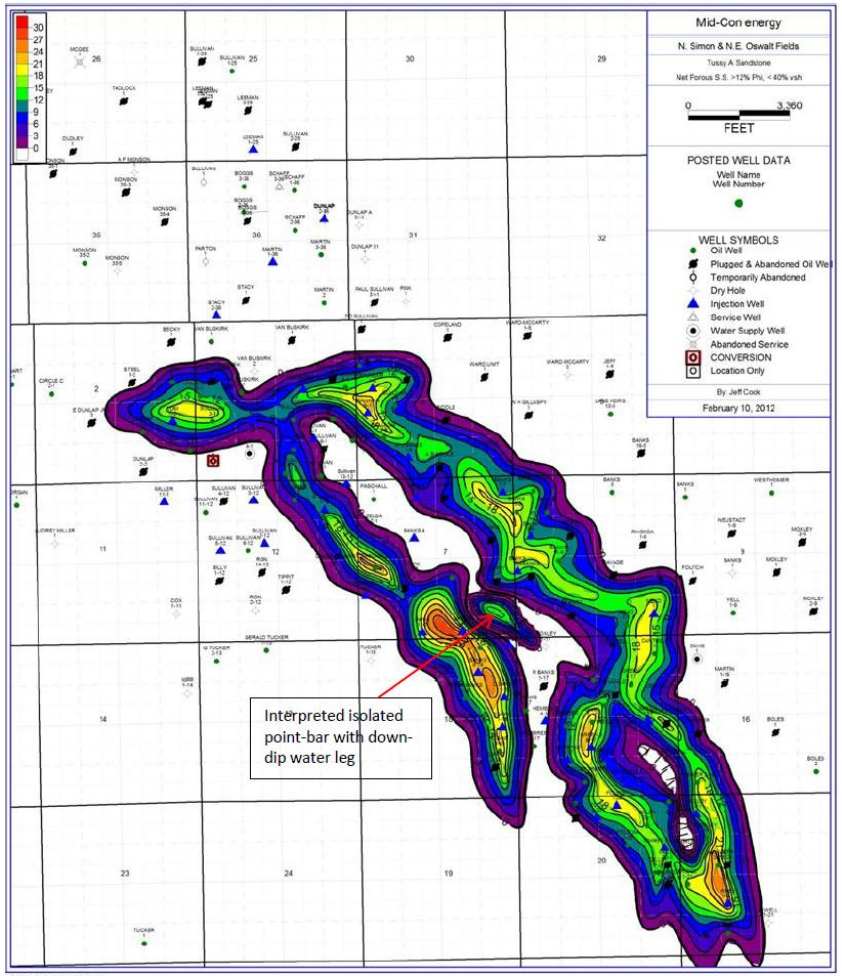


Figure 19. Thickness of net porous Tussy A Sandstone (density-neutron porosity > 12%; volume of shale < 40%). Contour interval: 3 ft. Thicknesses shown in color bar: zero (magenta) to 27 ft (red). Red arrow indicates oil-water contact within an interpreted disconnected sand body with a downdip water leg. Abandoned sand bodies of this type are the only observed oil-water contacts in the Tussy A Sandstone within the Southeast Joiner City field.

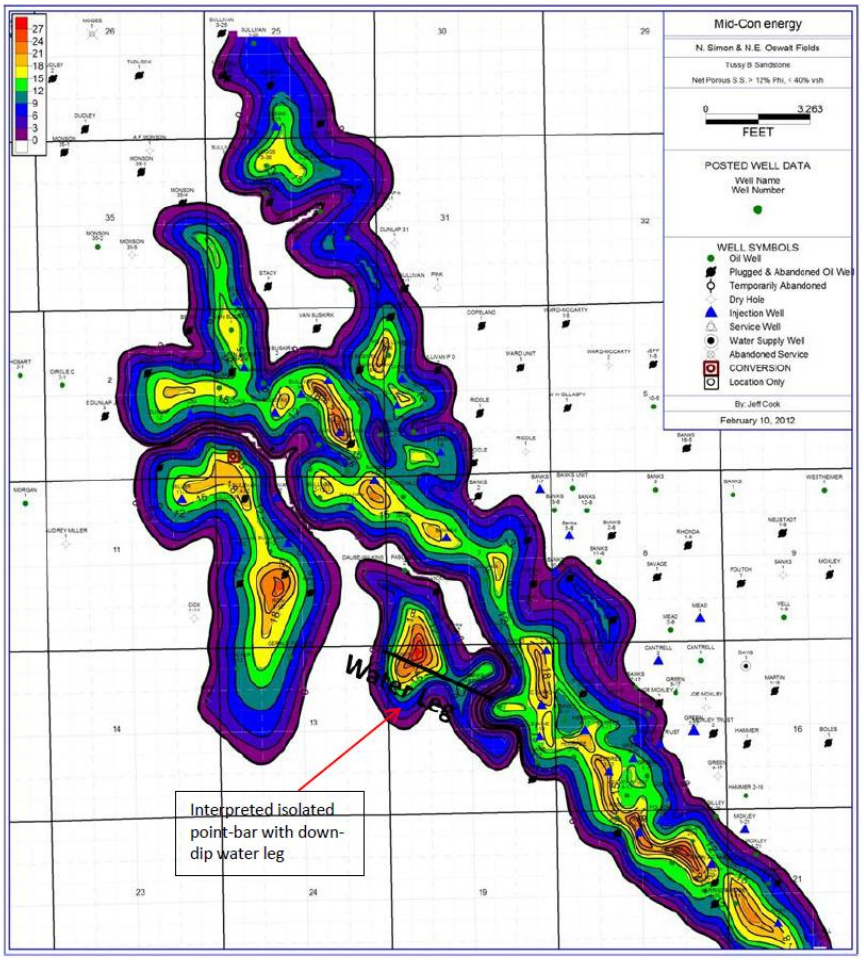


Figure 20. Thickness of net porous Tussy B Sandstone (density-neutron porosity > 12%; volume of shale < 40%). Contour interval: 3 ft. Thicknesses shown in color bar: zero (magenta) to 27 ft (red). Red arrow indicates oil-water contact within an interpreted disconnected sand body with a downdip water leg. Abandoned sand bodies of this type are the only observed oil-water contacts in the Tussy B Sandstone within the Southeast Joiner City field.

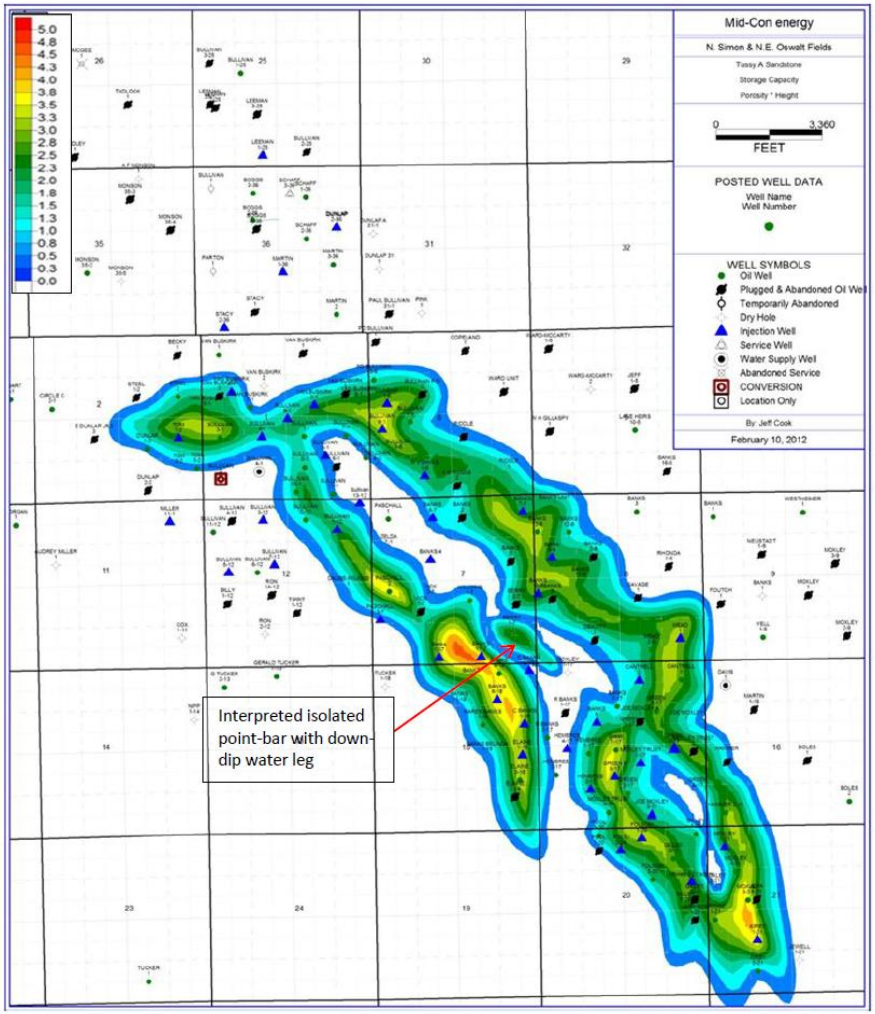


Figure 21. Storage-capacity thickness, Tussy A Sandstone. Storage capacity = average porosity x net-pay height. Contour interval and color bar are on left. Red arrow indicates a water leg in an isolated sandstone deposit.

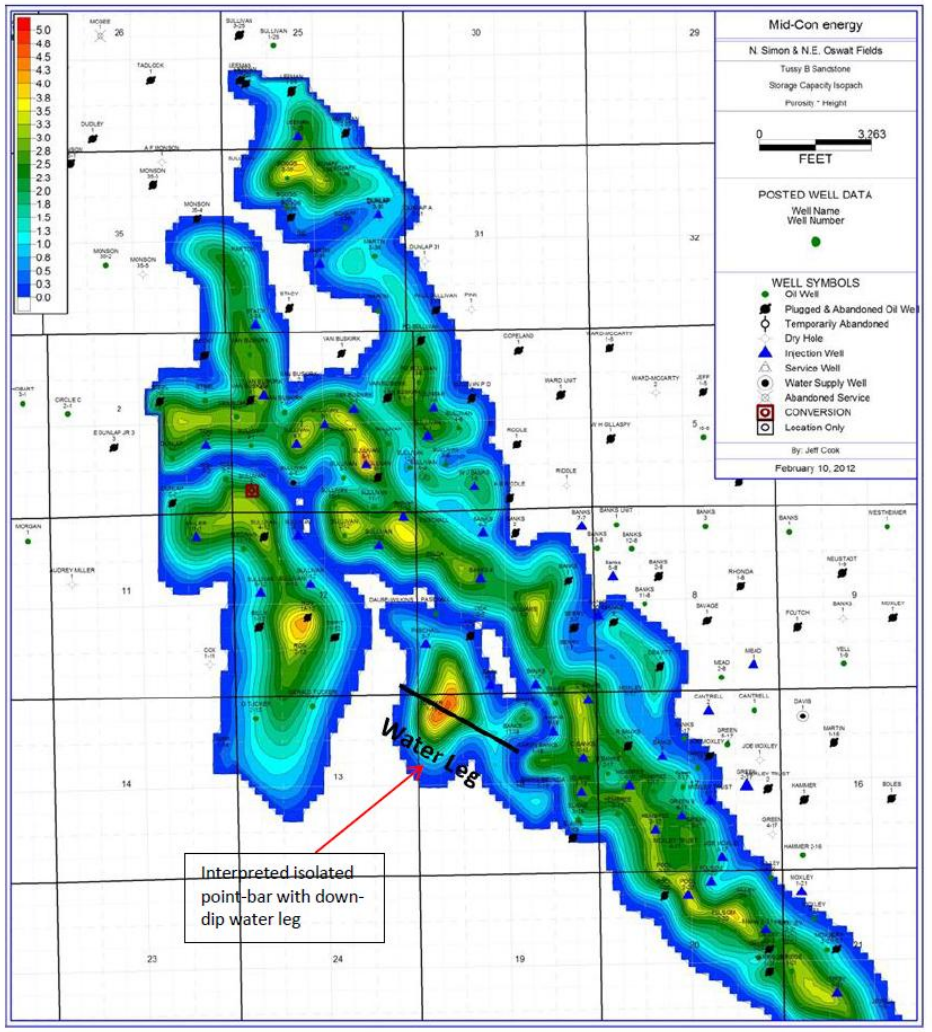


Figure 22. Storage-capacity thickness, Tussy B Sandstone. Storage capacity = average porosity x net pay height. Contour interval and color bar are on left. Black line indicates a water leg in an isolated sandstone deposit.

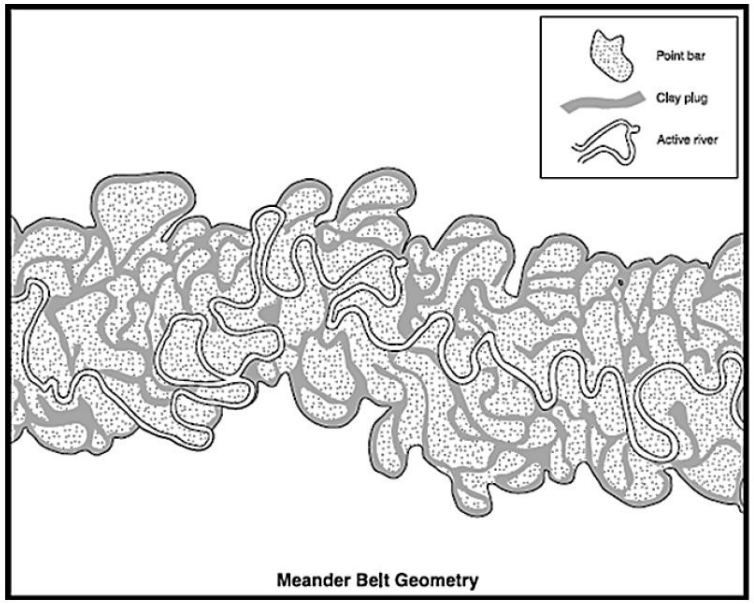


Figure 23. Computer simulation and model of a meander belt, showing prominent point bars (Sun et al., 1996).

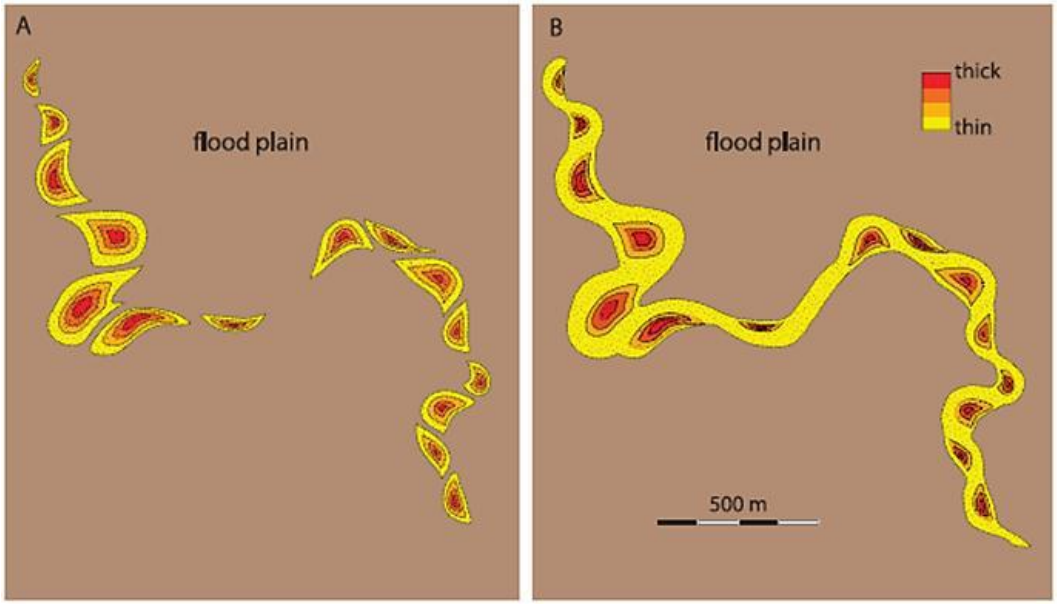


Figure 24. Isopach maps from Miocene Huesca fluvial fan in Ebro, Spain, showing two interpretations of meander - sandstone distribution and connectivity. (A) Fluvial channel is filled with mud after channel abandonment; point-bars are compartments. (B) Channel floor consists of clean trough-cross-bedded sand. The sand body is connected throughout the trend (Donselaar and Overeem, 2008).

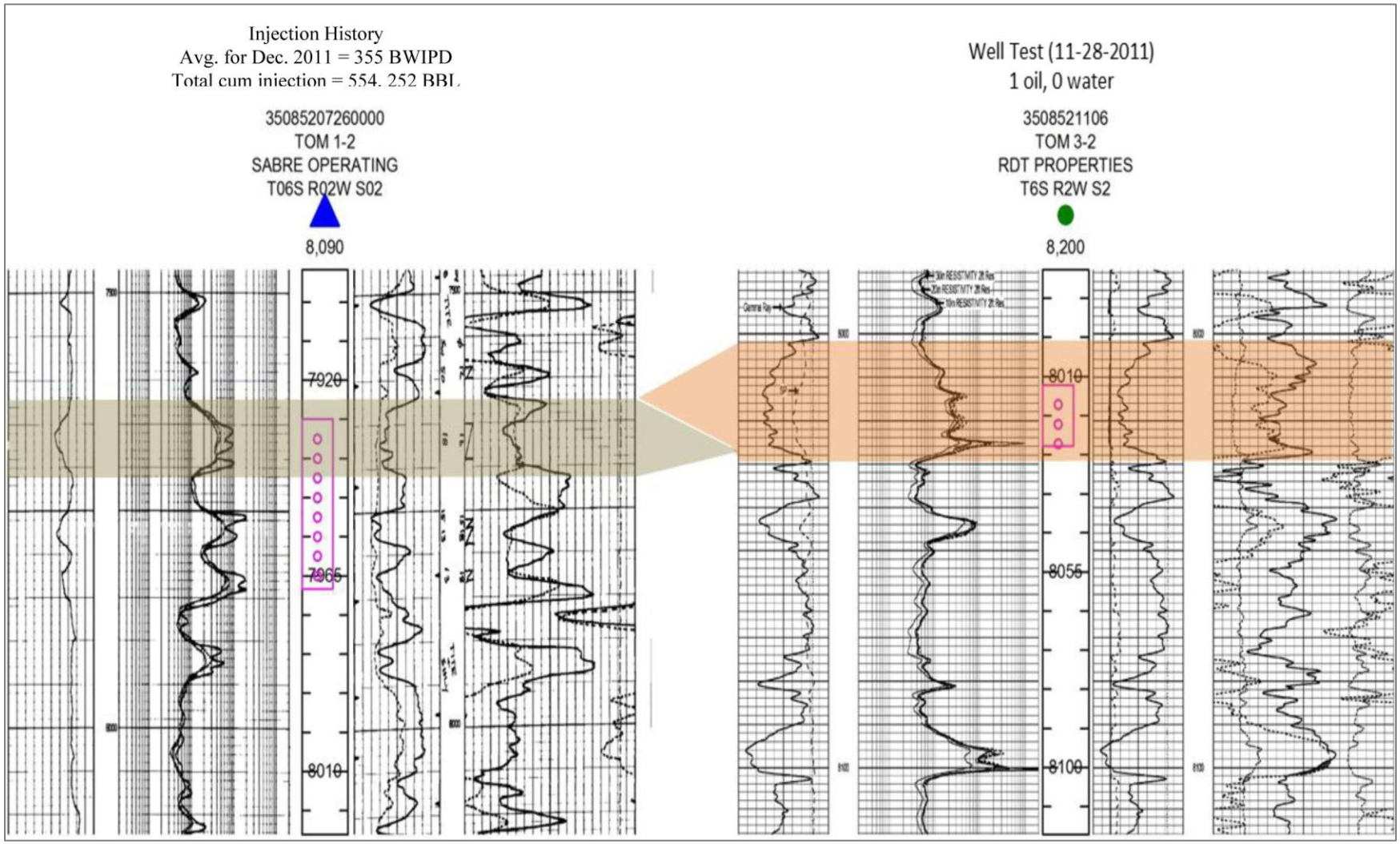


Figure 25. Log cross-section illustrating flow barriers between wells completed in the Tussy sandstones. The large volume of water injected into the Sabre Operating Tom 1-2 has caused no apparent increase in oil or water production from the RDT Tom 3-2, located only about 900 feet to the southeast. This flow baffle is consistent with inter-bar discontinuity in point-bar systems. Reference surface is Tussy Limestone.

## References Cited


Abbott, B.N., 2006, Pre-Pennsylvanian subcrop map, Love County, Oklahoma, unpublished map.

Al-Shaieb, Z.F., R.G. Thomas, and G.F. Stewart, 1980, National uranium resource evaluation, Lawton quadrangle, Oklahoma and Texas: U.S. Department of Energy, Open-File Report GJQ-0-17(82), 48 p.

Billingsley, P., S. Banerjee, R.D. Elmore, and P.K. Sutherland, 1996, Fluvial-deltaic facies patterns in the lower Deese Group (Middle Pennsylvanian), Ardmore Basin, *in* Johnson, K.S. (ed.), Deltaic Reservoirs in the Southern Midcontinent, 1993 Symposium: Oklahoma Geological Survey Circular 98, p. 240-248.

Boggs, S. Jr., 2006, Principles of Sedimentology and Stratigraphy, 4th edition: Pearson Prentice Hall – Pearson Education, Inc., 662 p.

Boyd, D.T., 2002, Map of Oklahoma oil and gas fields, Oklahoma Geological Survey Map GM-37.

Bradfield, H.H., 1968, Stratigraphy and structure of the deeper Marietta basin of Oklahoma and Texas, *in* W.J Stewart, editor, Basins of the Southwest, v. 1: North Texas Geological Society, p. 54-70

Cant, D.J., 1982, Fluvial facies models and their applications, *in* P.A. Scholle and D. Spearing, editors, Sandstone Depositional Environments: AAPG Memoir 31, p. 115-138.

Coleman, J.M., and D.B. Prior, 1982, Deltaic environments of deposition, *in* P.A. Scholle, and D. Spearing, editors., Sandstone Depositional Environments: AAPG Memoir 31, p. 139-178.

DeVries, A. A., 2005, Sequence stratigraphy and micro-image analysis of the Upper Morrow sandstone in the Mustang East field, Morton County Kansas: unpublished M.S. thesis, Oklahoma State University, Stillwater, Oklahoma

Donselaar, M. E., and I. Overeem, 2008, Connectivity of fluvial point-bar deposits: An example from the Miocene Huesca Fluvial Fan, Ebro Basin, Spain: AAPG Bulletin. v. 92/9, p. 1109-1129.

Feinstein, S., 1981, Subsidence and thermal history of southern Oklahoma aulacogen: Implications for petroleum exploration: AAPG Bulletin, v. 65/12, p. 2521-2533.

Ham, W.E., R.E. Denison, and C.A. Merritt, 1964, Basement rocks and structural evolution of southern Oklahoma: Oklahoma Geological Survey Bulletin 95, 302 p.

Hoard, J.L., 1954, Tussy Sector of the Tatums field, Carter, and Garvin Counties, Oklahoma: Petroleum Geology of Southern Oklahoma: A symposium: AAPG, v. 1, p. 186-206.

Mullen, L.M., 1954, The Hewitt Oil field of Carter County, Oklahoma: Petroleum Geology of Southern Oklahoma: A symposium: AAPG, v. 1, p. 154-161.

Neustadt, W. Jr., 1954, West Hewitt field, Carter County, Oklahoma: Petroleum Geology of Southern Oklahoma: A symposium: AAPG, v. 1, p. 162-173.

Rascoe, B. Jr., and F.J. Adler, 1983, Permo-Carboniferous hydrocarbon accumulations, Mid-Continent, U.S.A: AAPG Bulletin v. 62/6, p. 979-1001.

Reeves, C.C. Jr., and J.R. Mount, 1960, Possibility of hydrocarbon accumulations along northern flank of Marietta Syncline, Love County, Oklahoma, AAPG Bulletin, v. 44/1, p. 72-82.

Sun, T., P. Meakin, T. Jossang, and K. Schwarz, 1996, A simulation model of meandering rivers: Water Resources Research, v. 32, pt. 9, p. 2937-2954.

Tomlinson, C.W., and W. McBee, Jr., 1962, Pennsylvanian sediments and orogenies of Ardmore District, Oklahoma, *in* C.C. Branson, editor., Pennsylvanian System in the United States – a symposium: AAPG, p. 461-500.

Westheimer, J M., 1965, Geology and petroleum of Love County, Oklahoma: Part II-Petroleum geology of Love County, OGS Circular 63, 91 p.

## Acknowledgments

Grateful acknowledgments are to Mid-Con Energy Operating, Inc. (now Mid-Con Energy Partners, L.P.) for whom this research was done and for permission to publish the results of the study. Mid-Con provided the data for the study, and special thanks are extended to James McGhay, Randy Olmstead, Lisa Ingle, and Nick Abbott. Members of my thesis committee, Drs. James Puckette, Gary Stewart, and Darwin Boardman (deceased), provided guidance, advice, and recommendations. Special appreciation is expressed to my wife, Ashton Cook, for understanding and patience during the time of this study.